not always explain the organ specific metastasis, which is one of the important clinical features of bone metastasis. Recently, the host microenvironment has been demonstrated to be a niche for survival and growth of tumor cells [20,21]. Our "bone invasion model" has the limitation which does not recapitulate the entire process of bone metastasis, but focuses on the steps of survival and growth of the tumor in the bone microenvironment regardless of tumor type. Using our model, we identified a unique pattern of gene expression that was up-regulated at the TB interface, including genes such as RANKL, which are known to be involved in bone metastasis [31,32]. Therefore, this model provides an exciting opportunity to elucidate the molecular mechanisms underlying tumor stromal interaction in the bone microenvironment.

4. Role of RANKL in the bone microenvironment

We found that RANKL was up-regulated at the tumor bone interface in both prostate [29] and mammary models [29]. RANKL–RANK signaling is important in establishing bone metastasis because it is involved in activating the differentiation of preosteoclasts into activated osteoclasts, leading to bone resorption. This signal plays a central role in the vicious cycle [8], is up-regulated to establish osteolytic lesions.

Both RANKL and RANK proteins are bound to cell membrane. Consequently, in order to transduce RANKL–RANK signaling, physical cell-to-cell contact is required between RANKL expressing osteoblasts and RANK expressing osteoclast precursors. Since RANKL has been shown to be modulated by proteases [28,33,34], and we investigated the proteases, up-regulated at the TB-interface to determine whether they could modulate RANKL signaling to favor tumor progression. Using our prostate cancer model, we found that MMP-7 cleaved the extracellular domain of RANKL, generating an active soluble form of RANKL (sRANKL) that could activate osteoclasts and promote osteolysis using our prostate cancer model [28]. In addition, at the TB-interface of our mouse mammary tumor, we found cathepsin G, cathepsin K, matrix metalloproteinase (MMP)-9, and MMP-13 were up regulated [35], and we demonstrated that cathepsin G cleaved RANKL releasing sRANKL from the cell surface [35]. These results show that sRANKL generated by proteases in the bone microenvironment increases the number of activated osteoclasts, enhancing osteolysis. This suggests that sRANKL plays a critical role in widespread osteoclast activation in osteolytic lesions associated with bone metastatic tumors. Our data also demonstrate that proteases up-regulated in the bone microenvironment play an important role in inducing osteolytic lesions associated with the growth of metastatic tumors in the bone microenvironment by generating RANKL and contributing vicious cycle.

Interestingly, proliferation of lobulo-alveolar cells in the mammary grand during pregnancy is regulated by RANKL–RANK signaling [36] through activation of IκB kinase α (IKKα) [37]. This protein kinase also been demonstrated to be involved in proliferation of mammary cancer progenitors [38] and prostate [39] and breast cancer cells [40]. In a preliminary study, we demonstrated that RANKL inhibition led to decreased cell proliferation, which was associated with the suppression of phosphorylated IKK alpha (unpublished data). Taken together, RANKL–RANK signaling may regulate tumor cell proliferation as well as osteoclast induction in the bone microenvironment. These results suggest that sRANKL are potentially novel therapeutic target of bone metastasis of prostate and breast cancer.

5. Bone modifying agents targeting osteoclasts activity

Bone metastases associated with advanced stage prostate or breast cancer develops skeletal complications including bone pain, hypercalcemia, pathologic fracture, compression of the spinal cord, and spinal instability (also known as skeletal-related events, SREs) [41–43]. Progressive bone pain, in particular, can be severe and bothersome, as the effectiveness of analgesics, even opioid therapy is frequently declines [44–48]. The management of bone metastases can be accomplished by the combination of chemotherapy, radiation therapy and bone modifying agents such as bisphosphonate or RANKL antibody to prevent SREs [49].

Bone-modifying agents, denosumab, pamidronate, and zoledronic acid, are recommended for treatment of metastatic bone diseases [50]. Among them, zoledronic acid is approved for treatment of bone metastasis associated with castration resistant prostate cancer and denosumab has been shown to significantly increase metastasis-free survival of prostate cancer patients [51,52]. Clinical trials revealed that all these bone-modifying agents reduced the time to SRE, and SREs of breast cancer patients with bone metastasis [50]. Therefore, these agents are considered as the standard of care for reducing SREs of the patients with bone metastatic diseases [53–56]. However, the clinical trials also revealed that these bone modifying agents did not significantly prolonged the survival of the overall study population.

This has brought about a paradigm shift in the treatment of the patients, who need to preserve the quality of life (QOL) for an extended period of time because patients with metastatic disease are living longer due to improvements in cancer therapies for solid tumors. Thus, strategies in the management of metastatic bone diseases have been shifted to delay worsening of skeletal pain and aggravation of metastatic bone diseases. In fact, early palliative treatment enhanced the QOL in patients with metastatic lung cancer, which resulted in the reduction of the aggressive end-of-life care [57–59]. However, while this shift in management strategies and early intervention may improves patients' lives, these treatment do not address the specific issues of the patients with bone metastasis such as tumor dormancy, drug resistance, or improvement of survival.

6. CSC in the bone microenvironment

With the recent advent of cancer stem cell (CSC) theory, CSC activities has been identified in numerous solid tumors [60–67], including prostate [68], breast [69], and pancreas [70–72]. As discussed earlier, the process of metastasis is so inefficient that only a small subset of tumor cells that leave the primary site can successfully navigate the process of metastasis to re-initiate tumor growth to form macrometastases at distant sites.

The bone marrow regulates hematopoietic function. Hematopoietic stem cells (HSCs) are believed to localize to specific microenvironments in the bone marrow where regulation by osteoblasts, mesenchymal stem cells, adipocyctes, and CXCL12-abundant reticular (CAR) cells occurs [73–75]. In the marrow, quiescent HSCs have been demonstrated to preserve their capacity for self-renewal capable of dividing and differentiating to populate their corresponding lineages [76–78]. It is possible that such a niche would be good "soil" for CSC to grow in the bone microenvironment [79]. HSC regulating cells such as osteoblasts, bone marrow stromal cells and CAR cells may play a decisive role in maintaining CSCs in the bone microenvironment. In addition, CSCs may change the microenvironment into a more appropriate niche.

CSC is an attractive hypothesis for tumor development and progression, and coupled with the inherent tumor heterogeneity, CSCs could be involved in formation of metastases [80–84]. It is possible that CSCs in the bone microenvironment may explain the latency of bone metastasis formation, the very long period of time, a disseminated tumor cell in the bone microenvironment to grow into a gross metastasis [85]. Notably, the phenotype of a CSC may depend on the primary site and vary substantially across different microenvironments. Only CSCs specific to the bone microenvironment would contribute to bone metastasis formation. However, despite the convergence on the concept and intensive studies on CSCs, a single universal entity of CSCs was not clearly established, and the definition and identification of these cells remains elusive in most tumor types.

7. Summary and future directions

Despite significant improvements in local and systemic adjuvant therapies, bone metastases of prostate and breast cancer are still resistant to these therapies, which results in poor prognosis. Devastating skeletal complication develop in patients with bone metastatic diseases, which is the result of tumor stromal interaction in the bone microenvironment. Therapeutic agents targeting these interactions are required for management of these complications.

Strategies for the management of metastatic bone diseases have been shifted to delay worsening of skeletal pain and aggravation of metastatic bone diseases. Bone modifying agents, such as bisophosphonate and human RANKL antibody, are considered as the standard of care for reducing SREs of patients with bone metastatic diseases. However, new therapeutic agents need to be developed to prolong the survival of patients with bone metastatic diseases.

The process of metastasis is so inefficient that only a small subset of tumor cells that leave the primary site can successfully navigate the process of metastasis to form clinical metastases in the bone. Understanding the biology of the successful metastatic cell, which has some of the characteristics of the theoretical cancer stem cell in the bone microenvironment, should provide the opportunity of addressing specific issues such as tumor dormancy, and drug resistance. New treatment of bone metastatic diseases could be accomplished by the combination of bone modifying agents to prevent SREs and agents targeting homeostatic factors that preserve survival, growth of the tumor cells in the bone microenvironment.

Our understanding on the molecular and cellular interactions in the bone microenvironment is significantly improving and the development of effective therapies for bone metastasis is becoming even more realistic.

Disclosure statement

The authors have declared that no conflict of interest exists.

Acknowledgments

The authors would like to express gratitude to Dr. David B. Alexander, in Nanotoxicology Project, Nagoya City University, Nagoya, Japan, for discussion and comments on the manuscript. This work was supported in part by a research grant from the Scientific Support Programs for Cancer Research Grant-in-Aid for Scientific Research on Innovative Areas (221S0001) from Ministry of Education, Culture, Sports, Science, and Technology, and a grant-in-aid for Scientific Research (C, 15K06837) from the Japan Society for the Promotion of Science.

References

[1] I.J. Fidler, The pathogenesis of cancer metastasis: the 'seed and soil' hypothesis revisited, Nat. Rev. Cancer 3 (2003) 453–458.
[2] I.J. Fidler, Critical factors in the biology of human cancer metastasis, Am. Surg. 61 (1995) 1065–1066.
[3] V. Montel, T.Y. Huang, E. Mose, K. Pestonjamasp, D. Tarin, Expression profiling of primary tumors and matched lymphatic and lung metastases in a xenogeneic breast cancer model, Am. J. Pathol. 166 (2005) 1565–1579.
[4] T.P. Butler, P.M. Gullino, Quantitation of cell shedding into efferent blood of mammary adenocarcinoma, Cancer Res. 35 (1975) 512–516.
[5] I.J. Fidler, M.L. Kripke, Metastasis results from preexisting variant cells within a malignant tumor, Science 197 (1977) 893–895.
[6] I.J. Fidler, Metastasis: quantitative analysis of distribution and fate of tumor emboli labeled with 125 I-5-iodo-2′-deoxyuridine, J. Natl. Cancer Inst. 45 (1970) 773–782.
[7] I.J. Fidler, Biological behavior of malignant melanoma cells correlated to their survival *in vivo*, Cancer Res. 35 (1975) 218–224.
[8] G.R. Mundy, Metastasis to bone: causes, consequences and therapeutic opportunities, Nat. Rev. Cancer 2 (2002) 584–593.
[9] T.A. Guise, K.S. Mohammad, G. Clines, E.G. Stebbins, D.H. Wong, L.S. Higgins, R. Vessella, E. Corey, S. Padalecki, L. Suva, J.M. Chirgwin, Basic mechanisms responsible for osteolytic and osteoblastic bone metastases, Clin. Cancer Res. 12 (2006) 6213s–6216s.
[10] S.A. Charhon, M.C. Chapuy, E.E. Delvin, A. Valentin-Opran, C.M. Edouard, P.J. Meunier, Histomorphometric analysis of sclerotic bone metastases from prostatic carcinoma special reference to osteomalacia, Cancer 51 (1983) 918–924.
[11] A. Leibbrandt, J.M. Penninger, RANKL/RANK as key factors for osteoclast development and bone loss in arthropathies, Adv. Exp. Med. Biol. 649 (2009) 100–113.
[12] J.M. Delaisse, T.L. Andersen, M.T. Engsig, K. Henriksen, T. Troen, L. Blavier, Matrix metalloproteinases (MMP) and cathepsin K contribute differently to osteoclastic activities, Microsc. Res. Tech. 61 (2003) 504–513.
[13] B. Guo, D.J. Villeneuve, S.L. Hembruff, A.F. Kirwan, D.E. Blais, M. Bonin, A.M. Parissenti, Cross-resistance studies of isogenic drug-resistant breast tumor cell lines support recent clinical evidence suggesting that sensitivity to paclitaxel may be strongly compromised by prior doxorubicin exposure, Breast Cancer Res. Treat. 85 (2004) 31–51.
[14] Y. Kang, P.M. Siegel, W. Shu, M. Drobnjak, S.M. Kakonen, C. Cordon-Cardo, T.A. Guise, J. Massague, A multigenic program mediating breast cancer metastasis to bone, Cancer Cell 3 (2003) 537–549.
[15] C. Kuperwasser, S. Dessain, B.E. Bierbaum, D. Garnet, K. Sperandio, G.P. Gauvin, S.P. Naber, R.A. Weinberg, M. Rosenblatt, A mouse model of human breast cancer metastasis to human bone, Cancer Res. 65 (2005) 6130–6138.
[16] B.O. Murphy, S. Joshi, A. Kessinger, E. Reed, J.G. Sharp, A murine model of bone marrow micrometastasis in breast cancer, Clin. Exp. Metastasis 19 (2002) 561–569.
[17] J.A. Nemeth, J.F. Harb, U. Barroso Jr., Z. He, D.J. Grignon, M.L. Cher, Severe combined immunodeficient-hu model of human prostate cancer metastasis to human bone, Cancer Res. 59 (1999) 1987–1993.
[18] A.H. Reddi, D. Roodman, C. Freeman, S. Mohla, Mechanisms of tumor metastasis to the bone: challenges and opportunities, J. Bone Miner. Res. 18 (2003) 190–194.
[19] E. Shtivelman, R. Namikawa, Species-specific metastasis of human tumor cells in the severe combined immunodeficiency mouse engrafted with human tissue, Proc. Natl. Acad. Sci. U. S. A. 92 (1995) 4661–4665.
[20] S. Paget, The distribution of secondary growths in cancer of the breast. 1889, Cancer Metastasis Rev. 8 (1989) 98–101.
[21] S.A. Patel, M.A. Dave, R.G. Murthy, K.Y. Helmy, P. Rameshwar, Metastatic breast cancer cells in the bone marrow microenvironment: novel insights into oncoprotection, Oncol. Rev. 5 (2011) 93–102.
[22] V.A. Siclari, T.A. Guise, J.M. Chirgwin, Molecular interactions between breast cancer cells and the bone microenvironment drive skeletal metastases, Cancer Metastasis Rev. 25 (2006) 621–633.
[23] D. Luis-Ravelo, I. Anton, S. Vicent, I. Hernandez, K. Valencia, C. Zandueta, S. Martinez-Canarias, A. Gurpide, F. Lecanda, Tumor–stromal interactions of the bone microenvironment: *in vitro* findings and potential *in vivo* relevance in metastatic lung cancer models, Clin. Exp. Metastasis 28 (2011) 779–791.
[24] D.M. Sosnoski, V. Krishnan, W.J. Kraemer, C. Dunn-Lewis, A.M. Mastro, Changes in cytokines of the bone microenvironment during breast cancer metastasis, Int. J. Breast Cancer 2012 (2012) 160265.
[25] T. Yoneda, T. Hiraga, Crosstalk between cancer cells and bone microenvironment in bone metastasis, Biochem. Biophys. Res. Commun. 328 (2005) 679–687.
[26] T. Hiraga, A. Ueda, D. Tamura, K. Hata, F. Ikeda, P.J. Williams, T. Yoneda, Effects of oral UFT combined with or without zoledronic acid on bone metastasis in the 4T1/luc mouse breast cancer, Int. J. Cancer 106 (2003) 973–979.
[27] H. Iguchi, S. Tanaka, Y. Ozawa, T. Kashiwakuma, T. Kimura, T. Hiraga, H. Ozawa, A. Kono, An experimental model of bone metastasis by human lung cancer cells: the role of parathyroid hormone-related protein in bone metastasis, Cancer Res. 56 (1996) 4040–4043.
[28] C.C. Lynch, A. Hikosaka, H.B. Acuff, M.D. Martin, N. Kawai, R.K. Singh, T.C. Vargo-Gogola, J.L. Begtrup, T.E. Peterson, B. Fingleton, T. Shirai, L.M. Matrisian, M. Futakuchi, MMP-7 promotes prostate cancer-induced osteolysis *via* the solubilization of RANKL, Cancer Cell 7 (2005) 485–496.
[29] M. Futakuchi, K.C. Nannuru, M.L. Varney, A. Sadanandam, K. Nakao, K. Asai, T. Shirai, S.Y. Sato, R.K. Singh, Transforming growth factor-beta signaling at the tumor-bone interface promotes mammary tumor growth and osteoclast activation, Cancer Sci. 100 (2009) 71–81.
[30] M. Futakuchi, R.K. Singh, Animal model for mammary tumor growth in the bone microenvironment, Breast Cancer (Tokyo, Jpn.) 20 (2013) 195–203.
[31] T.J. Wilson, K.C. Nannuru, M. Futakuchi, R.K. Singh, Cathepsin G-mediated enhanced TGF-beta signaling promotes angiogenesis *via* upregulation of VEGF and MCP-1, Cancer Lett. 288 (2010) 162–169.
[32] A. Sadanandam, M. Futakuchi, C.A. Lyssiotis, W.J. Gibb, R.K. Singh, A cross-species analysis of a mouse model of breast cancer-specific osteolysis and human bone metastases using gene expression profiling, BMC Cancer 11 (2011) 304.
[33] T. Ohshiba, C. Miyaura, M. Inada, A. Ito, Role of RANKL-induced osteoclast formation and MMP-dependent matrix degradation in bone destruction by breast cancer metastasis, Br. J. Cancer 88 (2003) 1318–1326.
[34] E. Jimi, K. Aoki, H. Saito, F. D'Acquisto, M.J. May, I. Nakamura, T. Sudo, T. Kojima, F. Okamoto, H. Fukushima, K. Okabe, K. Ohya, S. Ghosh, Selective inhibition of NF-kappa B blocks osteoclastogenesis and prevents inflammatory bone destruction *in vivo*, Nat. Med. 10 (2004) 617–624.
[35] T.J. Wilson, K.C. Nannuru, M. Futakuchi, A. Sadanandam, R.K. Singh, Cathepsin G enhances mammary tumor-induced osteolysis by generating soluble receptor activator of nuclear factor-kappaB ligand, Cancer Res. 68 (2008) 5803–5811.
[36] J.E. Fata, Y.Y. Kong, J. Li, T. Sasaki, J. Irie-Sasaki, R.A. Moorehead, R. Elliott, S. Scully, E.B. Voura, D.L. Lacey, W.J. Boyle, R. Khokha, J.M. Penninger, The osteoclast differentiation factor osteoprotegerin-ligand is essential for mammary gland development, Cell 103 (2000) 41–50.

[37] Y. Cao, G. Bonizzi, T.N. Seagroves, F.R. Greten, R. Johnson, E.V. Schmidt, M. Karin, IKKalpha provides an essential link between RANK signaling and cyclin D1 expression during mammary gland development, Cell 107 (2001) 763–775.
[38] Y. Cao, J.L. Luo, M. Karin, IkappaB kinase alpha kinase activity is required for self-renewal of ErbB2/Her2-transformed mammary tumor-initiating cells, Proc. Natl. Acad. Sci. U. S. A. 104 (2007) 15852–15857.
[39] J.L. Luo, W. Tan, J.M. Ricono, O. Korchynskyi, M. Zhang, S.L. Gonias, D.A. Cheresh, M. Karin, Nuclear cytokine-activated IKKalpha controls prostate cancer metastasis by repressing Maspin, Nature 446 (2007) 690–694.
[40] W. Tan, W. Zhang, A. Strasner, S. Grivennikov, J.Q. Cheng, R.M. Hoffman, M. Karin, Tumour-infiltrating regulatory T cells stimulate mammary cancer metastasis through RANKL–RANK signalling, Nature 470 (2011) 548–553.
[41] R.E. Coleman, Future directions in the treatment and prevention of bone metastases, Am. J. Clin. Oncol. 25 (2002) S32–S38.
[42] R.E. Coleman, Clinical features of metastatic bone disease and risk of skeletal morbidity, Clin. Cancer Res. 12 (2006) 6243s–6249s.
[43] R.E. Coleman, R.D. Rubens, The clinical course of bone metastases from breast cancer, Br. J. Cancer 55 (1987) 61–66.
[44] C. Clare, D. Royle, K. Saharia, H. Pearse, S. Oxberry, K. Oakley, L. Allsopp, A.S. Rigby, M.J. Johnson, Painful bone metastases: a prospective observational cohort study, Palliat. Med. 19 (2005) 521–525.
[45] C.S. Cleeland, The measurement of pain from metastatic bone disease: capturing the patient's experience, Clin. Cancer Res. 12 (2006) 6236s–6242s.
[46] D.H. Henry, L. Costa, F. Goldwasser, V. Hirsh, V. Hungria, J. Prausova, G.V. Scagliotti, H. Sleeboom, A. Spencer, S. Vadhan-Raj, R. von Moos, W. Willenbacher, P.J. Woll, J. Wang, Q. Jiang, S. Jun, R. Dansey, H. Yeh, Randomized, double-blind study of denosumab *versus* zoledronic acid in the treatment of bone metastases in patients with advanced cancer (excluding breast and prostate cancer) or multiple myeloma, J. Clin. Oncol. 29 (2011) 1125–1132.
[47] W. Leppert, Pain management in patients with cancer: focus on opioid analgesics, Curr. Pain Headache Rep. 15 (2011) 271–279.
[48] A. Vainio, A. Auvinen, Prevalence of symptoms among patients with advanced cancer: an international collaborative study. Symptom Prevalence Group, J. Pain Symptom Manag. 12 (1996) 3–10.
[49] J.A. Dewar, Managing Metastatic Bone Pain, 2004.
[50] C.H. Van Poznak, S. Temin, G.C. Yee, N.A. Janjan, W.E. Barlow, J.S. Biermann, L.D. Bosserman, C. Geoghegan, B.E. Hillner, R.L. Theriault, D.S. Zuckerman, J.H. Von Roenn, O., American Society of Clinical Oncology executive summary of the clinical practice guideline update on the role of bone-modifying agents in metastatic breast cancer, J. Clin. Oncol. 29 (2011) 1221–1227.
[51] M.R. Smith, F. Saad, S. Oudard, N. Shore, K. Fizazi, P. Sieber, B. Tombal, R. Damiao, G. Marx, K. Miller, P. Van Veldhuizen, J. Morote, Z. Ye, R. Dansey, C. Goessl, Denosumab and bone metastasis-free survival in men with nonmetastatic castration-resistant prostate cancer: exploratory analyses by baseline prostate-specific antigen doubling time, J. Clin. Oncol. 31 (2013) 3800–3806.
[52] M.R. Smith, F. Saad, R. Coleman, N. Shore, K. Fizazi, B. Tombal, K. Miller, P. Sieber, L. Karsh, R. Damiao, T.L. Tammela, B. Egerdie, H. Van Poppel, J. Chin, J. Morote, F. Gomez-Veiga, T. Borkowski, Z. Ye, A. Kupic, R. Dansey, C. Goessl, Denosumab and bone-metastasis-free survival in men with castration-resistant prostate cancer: results of a phase 3, randomised, placebo-controlled trial, Lancet 379 (2012) 39–46.
[53] D.A. Berry, Biomarker studies and other difficult inferential problems: statistical caveats, Semin. Oncol. 34 (2007) S17–S22.
[54] I.P. Garraway, Targeting the RANKL pathway: putting the brakes on prostate cancer progression in bone, J. Clin. Oncol. 31 (2013) 3838–3840.
[55] F. Saad, J. Eastham, Zoledronic acid improves clinical outcomes when administered before onset of bone pain in patients with prostate cancer, Urology 76 (2010) 1175–1181.
[56] F. Saad, D.M. Gleason, R. Murray, S. Tchekmedyian, P. Venner, L. Lacombe, J.L. Chin, J.J. Vinholes, J.A. Goas, M. Zheng, Long-term efficacy of zoledronic acid for the prevention of skeletal complications in patients with metastatic hormone-refractory prostate cancer, J. Natl. Cancer Inst. 96 (2004) 879–882.
[57] B.E. Hillner, J.N. Ingle, J.R. Berenson, N.A. Janjan, K.S. Albain, A. Lipton, G. Yee, J.S. Biermann, R.T. Chlebowski, D.G. Pfister, American Society of Clinical Oncology guideline on the role of bisphosphonates in breast cancer. American Society of Clinical Oncology Bisphosphonates Expert Panel, J. Clin. Oncol. 18 (2000) 1378–1391.
[58] B.E. Hillner, J.N. Ingle, R.T. Chlebowski, J. Gralow, G.C. Yee, N.A. Janjan, J.A. Cauley, B.A. Blumenstein, K.S. Albain, A. Lipton, S. Brown, American Society of Clinical Oncology 2003 update on the role of bisphosphonates and bone health issues in women with breast cancer, J. Clin. Oncol. 21 (2003) 4042–4057.
[59] R. von Moos, F. Strasser, S. Gillessen, K. Zaugg, Metastatic bone pain: treatment options with an emphasis on bisphosphonates, Support. Care Cancer 16 (2008) 1105–1115.
[60] C.A. O'Brien, A. Pollett, S. Gallinger, J.E. Dick, A human colon cancer cell capable of initiating tumour growth in immunodeficient mice, Nature 445 (2007) 106–110.
[61] L. Ricci-Vitiani, D.G. Lombardi, E. Pilozzi, M. Biffoni, M. Todaro, C. Peschle, R. De Maria, Identification and expansion of human colon-cancer-initiating cells, Nature 445 (2007) 111–115.
[62] M.E. Prince, R. Sivanandan, A. Kaczorowski, G.T. Wolf, M.J. Kaplan, P. Dalerba, I.L. Weissman, M.F. Clarke, L.E. Ailles, Identification of a subpopulation of cells with cancer stem cell properties in head and neck squamous cell carcinoma, Proc. Natl. Acad. Sci. U. S. A. 104 (2007) 973–978.
[63] T. Schatton, G.F. Murphy, N.Y. Frank, K. Yamaura, A.M. Waaga-Gasser, M. Gasser, Q. Zhan, S. Jordan, L.M. Duncan, C. Weishaupt, R.C. Fuhlbrigge, T.S. Kupper, M.H. Sayegh, M.H. Frank, Identification of cells initiating human melanomas, Nature 451 (2008) 345–349.
[64] A. Eramo, F. Lotti, G. Sette, E. Pilozzi, M. Biffoni, A. Di Virgilio, C. Conticello, L. Ruco, C. Peschle, R. De Maria, Identification and expansion of the tumorigenic lung cancer stem cell population, Cell Death Differ. 15 (2008) 504–514.
[65] Z.F. Yang, D.W. Ho, M.N. Ng, C.K. Lau, W.C. Yu, P. Ngai, P.W. Chu, C.T. Lam, R.T. Poon, S.T. Fan, Significance of CD90+ cancer stem cells in human liver cancer, Cancer Cell 13 (2008) 153–166.
[66] S.K. Singh, C. Hawkins, I.D. Clarke, J.A. Squire, J. Bayani, T. Hide, R.M. Henkelman, M.D. Cusimano, P.B. Dirks, Identification of human brain tumour initiating cells, Nature 432 (2004) 396–401.
[67] M.D. Curley, V.A. Therrien, C.L. Cummings, P.A. Sergent, C.R. Koulouris, A.M. Friel, D.J. Roberts, M.V. Seiden, D.T. Scadden, B.R. Rueda, R. Foster, CD133 expression defines a tumor initiating cell population in primary human ovarian cancer, Stem Cells 27 (2009) 2875–2883.
[68] A.T. Collins, P.A. Berry, C. Hyde, M.J. Stower, N.J. Maitland, Prospective identification of tumorigenic prostate cancer stem cells, Cancer Res. 65 (2005) 10946–10951.
[69] M. Al-Hajj, M.S. Wicha, A. Benito-Hernandez, S.J. Morrison, M.F. Clarke, Prospective identification of tumorigenic breast cancer cells, Proc. Natl. Acad. Sci. U. S. A. 100 (2003) 3983–3988.
[70] R. Adikrisna, S. Tanaka, S. Muramatsu, A. Aihara, D. Ban, T. Ochiai, T. Irie, A. Kudo, N. Nakamura, S. Yamaoka, S. Arii, Identification of pancreatic cancer stem cells and selective toxicity of chemotherapeutic agents, Gastroenterology 143 (2012) 234–245 (e237).
[71] P.C. Hermann, S.L. Huber, T. Herrler, A. Aicher, J.W. Ellwart, M. Guba, C.J. Bruns, C. Heeschen, Distinct populations of cancer stem cells determine tumor growth and metastatic activity in human pancreatic cancer, Cell Stem Cell 1 (2007) 313–323.
[72] C. Li, D.G. Heidt, P. Dalerba, C.F. Burant, L. Zhang, V. Adsay, M. Wicha, M.F. Clarke, D.M. Simeone, Identification of pancreatic cancer stem cells, Cancer Res. 67 (2007) 1030–1037.
[73] Y. Shiozawa, A.M. Havens, K.J. Pienta, R.S. Taichman, The bone marrow niche: habitat to hematopoietic and mesenchymal stem cells, and unwitting host to molecular parasites, Leukemia 22 (2008) 941–950.
[74] T. Sugiyama, H. Kohara, M. Noda, T. Nagasawa, Maintenance of the hematopoietic stem cell pool by CXCL12-CXCR4 chemokine signaling in bone marrow stromal cell niches, Immunity 25 (2006) 977–988.
[75] R.S. Taichman, M.J. Reilly, S.G. Emerson, Human osteoblasts support human hematopoietic progenitor cells *in vitro* bone marrow cultures, Blood 87 (1996) 518–524.
[76] D.N. Haylock, S.K. Nilsson, Stem cell regulation by the hematopoietic stem cell niche, Cell Cycle 4 (2005) 1353–1355.
[77] R.S. Taichman, Blood and bone: two tissues whose fates are intertwined to create the hematopoietic stem-cell niche, Blood 105 (2005) 2631–2639.
[78] J. Zhu, S.G. Emerson, A new bone to pick: osteoblasts and the haematopoietic stem-cell niche, Bioessays 26 (2004) 595–599.
[79] R.N. Kaplan, R.D. Riba, S. Zacharoulis, A.H. Bramley, L. Vincent, C. Costa, D.D. MacDonald, D.K. Jin, K. Shido, S.A. Kerns, Z. Zhu, D. Hicklin, Y. Wu, J.L. Port, N. Altorki, E.R. Port, D. Ruggero, S.V. Shmelkov, K.K. Jensen, S. Rafii, D. Lyden, VEGFR1-positive haematopoietic bone marrow progenitors initiate the pre-metastatic niche, Nature 438 (2005) 820–827.
[80] L.L. Campbell, K. Polyak, Breast tumor heterogeneity: cancer stem cells or clonal evolution? Cell Cycle 6 (2007) 2332–2338.
[81] M.F. Clarke, J.E. Dick, P.B. Dirks, C.J. Eaves, C.H. Jamieson, D.L. Jones, J. Visvader, I.L. Weissman, G.M. Wahl, Cancer stem cells—perspectives on current status and future directions: AACR workshop on cancer stem cells, Cancer Res. 66 (2006) 9339–9344.
[82] S.A. Stacker, M.E. Baldwin, M.G. Achen, The role of tumor lymphangiogenesis in metastatic spread, FASEB J. 16 (2002) 922–934.
[83] S.S. Sundar, T.S. Ganesan, Role of lymphangiogenesis in cancer, J. Clin. Oncol. 25 (2007) 4298–4307.
[84] I. Van der Auwera, Y. Cao, J.C. Tille, M.S. Pepper, D.G. Jackson, S.B. Fox, A.L. Harris, L.Y. Dirix, P.B. Vermeulen, First international consensus on the methodology of lymphangiogenesis quantification in solid human tumours, Br. J. Cancer 95 (2006) 1611–1625.
[85] F. Li, B. Tiede, J. Massague, Y. Kang, Beyond tumorigenesis: cancer stem cells in metastasis, Cell Res. 17 (2007) 3–14.

Microbiology and Immunology

Microbiol Immunol 2016; 60: 35–46
doi: 10.1111/1348-0421.12338

ORIGINAL ARTICLE

C5a inhibitor protects against ischemia/reperfusion injury in rat small intestine

Eszter Tuboly[1], Mitsuru Futakuchi[2], Gabriella Varga[1], Daniel Érces[1], Tünde Tőkés[1], Andras Mészáros[1], József Kaszaki[1], Masumi Suzui[2], Masaki Imai[3], Alan Okada[4], Noriko Okada[5], Mihály Boros[1] and Hidechika Okada[5,*]

[1]Institute of Surgical Research, Faculty of Medicine, University of Szeged, 6 Szőkefalvi-Nagy Béla Street, Szeged, 6720, Hungary, [2]Department of Molecular Toxicology, [3]Department of Immunology, Graduate School of Medical Sciences, Nagoya City University, 1-Kawasumi, Mizuho-cho, Mizuho-ku, Nagoya, 467-8601, [4]Research Institute for Protein Science, 2-18 Nakayama-cho, Mizuho-ku, Nagoya, 467-0803, Japan and [5]Professor Emeritus, Nagoya City University

ABSTRACT

Acute mesenteric ischemia (AMI) is caused by considerable intestinal injury, which is associated with intestinal ischemia followed by reperfusion. To elucidate the mechanisms of ischemia/reperfusion injuries, a C5a inhibitory peptide termed AcPepA was used to examine the role of C5a anaphylatoxin, induction of inflammatory cells, and cell proliferation of the intestinal epithelial cells in an experimental AMI model. In this rat model, the superior mesenteric artery was occluded and subsequently reperfused (Induce-I/R). Other groups were treated with AcPepA before ischemia or reperfusion. Induce-I/R induced injuries in the intestine and AcPepA significantly decreased the proportion of severely injured villi. Induce-I/R induced secondary receptor for C5a-positive polymorphonuclear leukocytes in the vessels and CD204-positive macrophages near the injured site; this was correlated with hypoxia-induced factor 1-alpha-positive cells. Induction of these inflammatory cells was attenuated by AcPepA. In addition, AcPepA increased proliferation of epithelial cells in the villi, possibly preventing further damage. Therefore, Induce-I/R activates C5a followed by the accumulation of polymorphonuclear leukocyte and hypoxia-induced factor 1-alpha-producing macrophages, leading to villus injury. AcPepA, a C5a inhibitory peptide, blocks the deleterious effects of C5a, indicating it has a therapeutic effect on the inflammatory consequences of experimental AMI.

Key words complement C5a, hypoxia-induced factor 1-alpha, ischemia, macrophage.

Acute mesenteric ischemia, a critical circulatory condition, is caused by an arterial or venous thrombosis or embolism (1, 2). The overall mortality rate of AMI has remained at 60% to 80% over the last 25 years and the incidence of this disease is increasing (3, 4). AMI comprises a group of pathologic processes that have a common end point—intestinal necrosis (4). The intestinal epithelium is probably one of the most sensitive tissues to I/R injury in the body (5); intestinal ischemia rapidly progresses to severe metabolic derangements, infiltration of inflammatory cells, loss of villi and epithelial cells, and mucosal destruction, culminating in irreversible bowel necrosis (3).

Reoxygenation is crucial for cell survival, however, it has been well established that I/R causes much more

Correspondence
Mitsuru Futakuchi, Department of Molecular Toxicology, Graduate School of Medical Sciences, Nagoya City University, 1-Kawasumi, Mizuho-cho, Mizuho-ku, Nagoya, 467-8601, Japan. Tel:+81-52-853-8992, fax: +81-52-853-8996; email: futakuch@med.nagoya-cu.ac.jp

*Present address: Research Institute for Protein Science, Nakayama-cho 2-18, Mizuho-ku, Nagoya 467-0803, Japan

Received 9 November 2015; accepted 11 November 2015.

List of Abbreviations: AMI, acute mesenteric ischemia; C5L2, secondary receptor for C5a; CD68+MAC, CD68-positive macrophage; CD204+MAC, CD204-positive macrophage; HIF-1α, hypoxia-induced factor 1-alpha; IHC, immunohistochemical staining; I/R, Intestinal ischemia followed by reperfusion; Induce-I/R, induction of intestinal ischemia; Induce-I/R, induction of intestinal ischemia followed by reperfusion; PCNA, proliferating cell nuclear antigen; PMN, polymorphonuclear leukocyte.

severe tissue injury than that induced by ischemia alone (6). Investigation of the development of I/R damage has revealed significant regeneration of the mucosa, which parallels necrosis and apoptosis of the epithelial cells of the villi (7, 8). Published studies have suggested that I/R injury involves multiple processes, including activation of inflammatory cells with cytokine production followed by decay or regeneration of the injured epithelial cells. A variety of endogenous compounds and effector cells have been identified as mediators of I/R injury, including platelet-activating factor (9), TNF-α (10), IL-6 (11) and oxygen radicals (12). It is also well-known that I/R induces the so-called antigen-independent inflammatory pathway via which cellular and molecular participants of the immune system can be activated (13).

The complement system has been implicated as a major candidate in I/R injury, several studies having suggested that complement activation is involved in I/R injury in the gut (14–16). Complement activation results in production of C5a, which has been shown to be fundamental in exacerbation of I/R injuries (17). Complement activation occurs in the early stages of inflammation. In the case of gut I/R, activated complement induces activation of inflammatory cells, such as PMNs and macrophages, which have been demonstrated to play central roles in the development of I/R injury (18–20). In addition, C5a has been demonstrated to enhance the release of a number of pro-inflammatory cytokines from activated PMNs and macrophages (21–23). Furthermore, inhibition of C5a by a complementary peptide to C5a (AcPepA) reportedly suppresses the release of high mobility group box 1 resulting in rescue of monkeys injected with lethal doses of LPS (24).

C5a is considered to be a major factor in complement-mediated I/R tissue injury. Thus, the development of I/R injury involves multiple processes, such as C5a generation, induction of inflammatory cells and cytokine production, all of which lead to apoptosis and regeneration of the injured intestinal epithelial cells. These processes would involve cellular and molecular cross-talk among inflammatory cells, which has not yet been investigated in detail. C5a is believed to be a major factor in complement-mediated I/R tissue injury. Accordingly, the present study aimed to shed more light on the possible cellular and molecular pathways involved in the proliferative consequences of I/R events.

To this end we used AcPepA, which we have generated as an inhibitory complementary peptide (C-peps) of C5a (25–27) and examined its modulating effects on certain inflammatory responses, such as induction of C5L2-positive cells, induction of activated macrophages and involvement of HIF1-α in I/R injury, in a clinically relevant animal model of AMI.

MATERIALS AND METHODS

Animals and surgical preparation

The experiments were performed in full accordance with the National Institutes of Health guidelines on the handling and care of experimental animals and the study was approved by the Animal Welfare Committee of the University of Szeged.

A total of 35 male Sprague–Dawley rats (250–350 g body weight) were anesthetized with sodium pentobarbital (50 mg/kg, intraperitoneally) and placed in a supine position on a heating pad. Tracheostomy was performed to facilitate spontaneous breathing, after which the right jugular vein was cannulated with PE50 tubing for administration of Ringer's lactate infusion (10 mL/kg/hr) and to facilitate maintenance of anesthesia with sodium pentobarbital throughout the experiment.

The right common carotid artery was cannulated to measure the mean arterial pressure, which was measured at 30-min intervals and monitored throughout the investigation. The i.v. administration of AcPepA did not influence the mean arterial pressure of any of the treated animals (data not shown).

Experimental protocol

After confirming cardiovascular stabilization during the 30-minute recovery from anesthesia, a median laparotomy was performed to carry out the following experimental protocol. The animals were divided into five groups. Rats in group A served as a sham-operated group ($n=5$). Rats in groups B ($n=8$) and C ($n=8$), were exposed to ischemic insult, in which the superior mesenteric artery was occluded for 45 min with an atraumatic vascular clamp (Induce-I). Rats in groups D ($n=7$) and E ($n=7$), were subjected to ischemia followed by reperfusion for 30 min (Induce-I/R). Rats in groups C and E were given AcPepA (courtesy of Alan Okada, Research Institute for Protein Science, Nagoya, Japan) (4 mg/kg iv. in Ringer's lactate solution) 30 min after initiation of ischemia. The tissue samples were divided into two portions. One was used for histological and immunohistochemical analyses, whereas the other served as materials for proteomic investigation and was stored at −70°C. For histology, samples were fixed with 4% paraformaldehyde and then embedded and processed for further analysis. The fixed tissue was attached to hard backing with staples to ensure the optimal longitudinal orientation of the section.

Evaluation of the degree of injury to the villi

To evaluate the effects of ischemia, I/R and AcPepA treatment on small intestinal villi, the percentage of injured villi was calculated for each animal. The total number of villi in each hematoxylin and eosin-stained section was counted (20–25 fields at 400× magnification). Each villus was assigned to one of four categories (uninjured, slight, moderate or severe), depending on the degree of damage (length of the villus, infiltration of inflammatory cells, presence of surface erosion and amount of necrotic epithelium in the lumen).

In vivo detection of structural damage

The extent of microvascular and epithelial damage in the terminal ileum was evaluated by fluorescence real-time laser scanning confocal endomicroscopy (Five1, Ex. 488 nm, Em. 505–585 nm; Optiscan, Melbourne, Victoria, Australia) 30 min after the beginning of reperfusion. The mucosal surface of the terminal ileum was surgically exposed 5 cm proximal to the cecum and laid flat for examination. The microvascular structure was recorded after i.v. administration of 0.3 mL of fluorescein isothiocyanate-dextran (150 kDa, Sigma-Aldrich, St. Louis, Missouri, USA, 20 mg mL^{-1} solution dissolved in physiological saline). Confocal imaging was performed 5 min after dye administration (one scan/image, 1024×512 pixels and 475×475 μm per image). The villous architecture was examined following topical application of the fluorescent dye acridine orange (Sigma-Aldrich), surplus dye being flushed away from the mucosal surface of the ileum with physiological saline 2 min before imaging.

Immunohistochemical analysis

CD68 receptor, PCNA, C5L2 and CD204 receptors and HIF-1α expression were evaluated by IHC of sections of the small intestine. For this IHC study, the following diluted primary antibodies were prepared: PCNA (Clone PC10, 1:500; Dako Japan., Tokyo, Japan), C5L2 (1:100; kindly provided by Masaki Imai, Department of Immunology, Nagoya City University, Nagoya, Japan), CD68 primary antibody (1:100; BMA Biomedicals, Augst, Switzerland), CD204 (1:100; Trans Genic, Kumamoto, Japan), and HIF1-α (1:100; Thermo Fisher Scientific, Cheshire, UK). The entire IHC investigation was carried out using an automatic IHC machine, Leica Bond-max (Leica Microsystems, Tokyo, Japan) according to the manufacturer's instructions. For quantitative analysis, immunostained sections were examined under a light microscope, and the numbers of nuclei and cells positive for PCNA, C5L2, CD68, CD204 and HIF1-α enumerated at a magnification of ×400 for each region of the normal and injured villi, respectively.

Statistical analysis

Statistical analysis of the *in vivo* data was performed using Kruskal–Wallis and Bonferroni/Dunn multiple comparison tests. Data are presented as means ± SD. Values of $P < 0.05$ were deemed significant.

RESULTS

Effect of AcPepA on the degree of small intestinal injury

Induce-I and Induce-I/R induced various degrees of injury to the small intestine. The villi were sorted into four categories: uninjured (Fig. 1a), slightly (Fig. 1b), moderately (Fig. 1c) and severely injured (Fig. 1d), based on various histological criteria. About 96% of the intestinal villi in the control group were classified as uninjured (Table 1). The degrees of injury to the villi induced by Induce-I and Induce-I/R are shown in Table 1. The proportion of severely injured villi in the Induce-I/R group (76%) was significantly higher than that in the Induce-I group (6%) and was significantly reduced by AcPepA administration (to 24%; Table 1, Figure 1e).

Because Induce-I/R caused more severe injury to the small intestinal epithelium (76%) than did Induce-I (6%), the surface and micro-vessels of the small intestinal villi were further examined by confocal laser scanning endomicroscopy. Acridine orange staining revealed that the surfaces of the villi in the control group were smooth (Fig. 1f). Although longitudinal fissures and epithelial gaps filled with tissue debris were observed in the Induce-I/R group (Fig. 1g), only a few shed cells and epithelial gaps were observed in the AcPepA administration following Induce-I/R group (Figure 1h). Similarly, microvessel structures observed in the control group (Fig. 1i) were disorganized and fluorescent dye leakage was recorded in several areas of small intestinal villi (Fig. 1j). The extent of leakage was diminished by AcPepA administration following Induce-I/R (Fig. 1k). Thus, AcPepA treatment significantly reduced the degree of microvascular damage and preserved the epithelial morphology.

Taken together, these results suggest that Induce-I/R causes more severe injury to the small intestinal epithelium than does Treat-I alone, indicating that C5a activation may be involved in the increased damage that can be suppressed by the C5a-inhibitory peptide AcPepA.

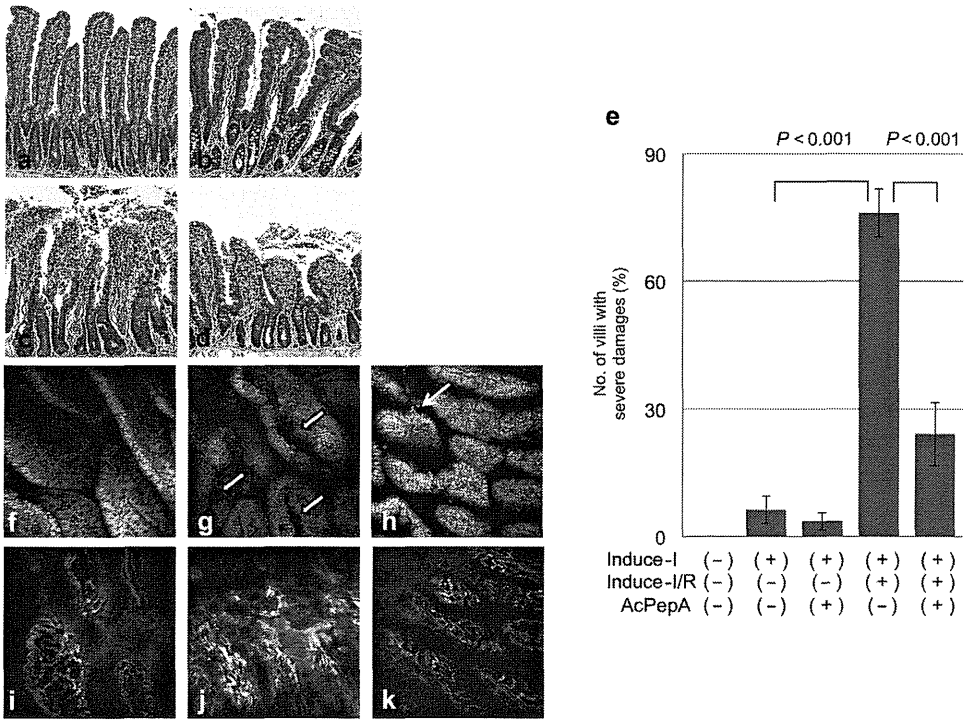

Fig. 1. Effect of AcPepA on the degree of small intestinal injury. Small intestinal injury (×600) was classified as (a) normal, (b) slight, (c) moderate and (d) severe. (e) The percentages of severely injured villi in the variously treated groups. *In vivo* histology images of the mucosal surface of distal rat ileum recorded under fluorescence confocal endomicroscopy (f, g, h) after i.v. administration of FITC-dextran and (i, j, k) topical administration of acridine orange. (f) Normal epithelium on the surface of the villi of the control group. (g) Longitudinal fissures on the surface of villi (white arrows) are apparent in the Induce-I/R group. (h) A few fissures on the surface of villi (thin white arrow) were observed in the Induce-I/R + AcPepA group. (i) Mucosal vasculature was normal in the control group. (j) Severe dye leakage from vessel lumina was observed 30 min after reperfusion in the Induce-I/R group. (k) Little dye leakage was observed in the Induce-I/R + AcPepA group.

Effects of AcPepA administration on proliferative changes in the epithelium with Induce-I/R

Because injuries to the small intestine change the resulted in a distributed balance between proliferation and apoptosis in the epithelium, the extent of proliferation of epithelial cells in the villi (except in strongly proliferative lesions) was examined to enable detection of small differences in the proliferation index (Fig. 2a). In normal villi, the PCNA index of the epithelium was 0.6–0.8% regardless of the treatment (Fig. 2b, c). In the injured villi, PCNA indices in the Induce-I group were similar to those observed in the Induce-I + AcPepA as well as in the Induce-I/R group (Fig. 2c). Administering AcPepA following Induce-I/R significantly increased the PCNA index compared with Induce-I/R without AcPepA administration (Fig. 2d, f). These results indicate that C5a inhibition by AcPepA alleviates I/R injury and increases cell proliferation in the epithelium.

Table 1. Degree of damage observed in intestinal villi

Intervention	No. of villi examined	No. of damaged villi (%)			
		Uninjured	Slightly	Moderately	Severely
Control	266	96	4	0	0
Induce-I	413	3	25	66	6
Induce-I + AcPep	436	2	47	47	4
Induce-I/R	289	0	2	22	76†
Induce-I/R + AcPep	417	0	14	62	24‡

†, $P < 0.001$ versus Induce-I/R
‡, $P < 0.001$ versus Induce-I

Induction of C5L2-positive PMNs in the villi

The localization of C5L2, a C5a receptor, was analyzed to identify cells in which C5a/C5L2 signaling is possibly transduced. Circulating inflammatory cells were often observed in dilated vessels located in the centers of villi, this phenomenon being associated with an inflammatory

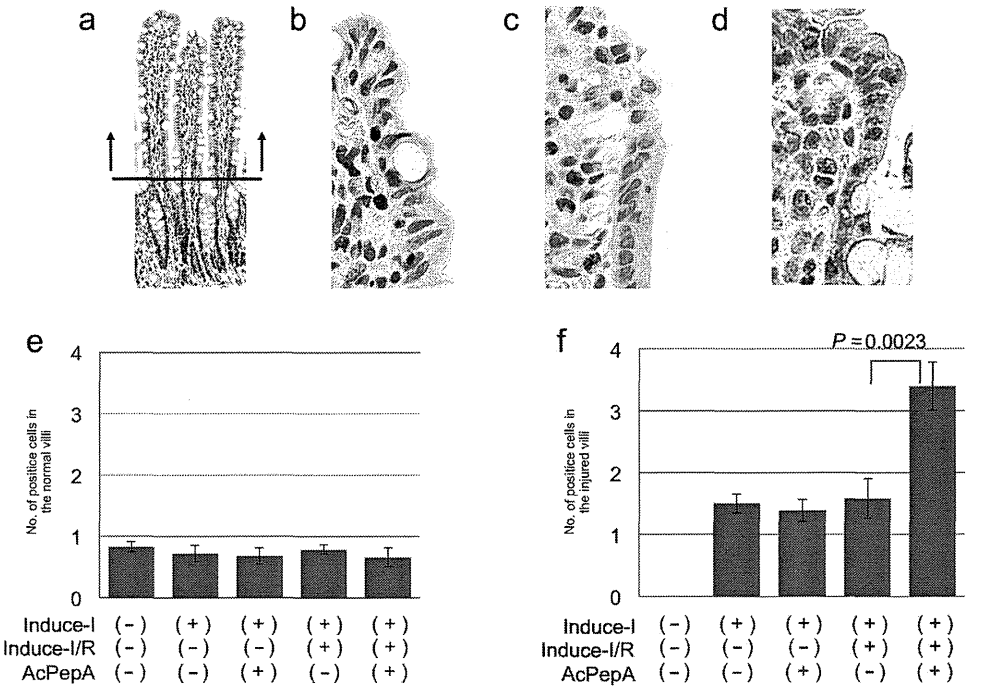

Fig. 2. Effect of AcPepA on proliferation of small intestinal epithelium. Recovery of the epithelium was evaluated by cell proliferation by counting PCNA-positive cells (PCNA index). (a) Positive epithelial cells were counted in the villi to avoid the strong proliferative region (below the horizontal bar in [a]) to facilitate detection of small differences in the cell proliferation index. Epithelial cells of injured small intestinal villi were visualized by PCNA staining of tissue from rats in the (b) Induce-I alone, (c) Induce-I/R and (d) Induce-I/R + AcPepA groups. (e) PCNA indices (number of positive cells in each villus) of the epithelium of normal and (f) injured villi are summarized.

response (square in Fig. 3a). C5L2-positive cells were observed among PMNs in the vessels (Fig. 3b). A few positive cells were observed outside the vessels such as in the erosion front of the injured villi (data not shown). $C5L2^{+}$PMNs were also observed in the dilated vessels of moderately or severely injured villi (Fig. 3c, d). The average number of $C5L2^{+}$PMNs was less than one in both the control and uninjured villi groups (Fig. 3E), the number of $C5L2^{+}$PMNs in the injured villi of the Induce-I/R group was significantly higher than in the Induce-I group. Additionally, $C5L2^{+}$PMNs were remarkably reduced by AcPepA administration in the Induce-I/R group (Fig. 3f). Because of our observation of a drastic increase in the number of C5L2-positive cells in vessels of the villi of the Induce-I/R group, C5a concentrations in the sera of the control, Induce-I/R and Induce-I/R + AcPepA groups were examined next (Fig. 3g). The serum concentration of C5a was 12 ng/mL in the control group, whereas in the Induce-I and Induce-I/R groups it was undetectable (Fig. 3g). An additional treatment with AcPepA restored the C5a concentration to >12 ng/mL, which is equivalent to that of the control group (Fig. 3g). These results suggest that C5a stimulates $C5L2^{+}$PMNs, causing a release of cytokines which exacerbate inflammation; thus, $C5L2^{+}$PMNs may contribute indirectly to I/R injury. Although Induce-I alone completely exhausted C5a in serum, Induce-I/R increased the C5a concentration up to 5 ng/mL, this possibly being attributable to further generation of C5a by reperfusion (R) following ischemia (I). The increased concentration of C5a (over 12 ng/mL) in rats treated with AcPepA following Induce-I/R may indicate protection of C5 by AcPepA from catabolism by an inhibitor of C5a, namely carboxypeptidase R (28, 29), which is also known as thrombin activatable fibrinolysis inhibitor.

Induction of CD68-positive macrophages in the villi

Next, evidence of macrophage induction in the control and injured villi was examined. In contrast with C5L2+PMNs, most CD68+MACs were observed in stromal lesions outside the vessels in slightly injured villi (arrowheads in Figure 4a). CD68+MACs were observed in the erosion fronts of the injured villi (arrowheads in Fig. 4b). Although many macrophages were observed with Induce-I/R (Fig. 4b), fewer were observed with Induce-I/R + AcPepA (Figure 4c). Regardless of the form of treatment, about one macrophage was observed

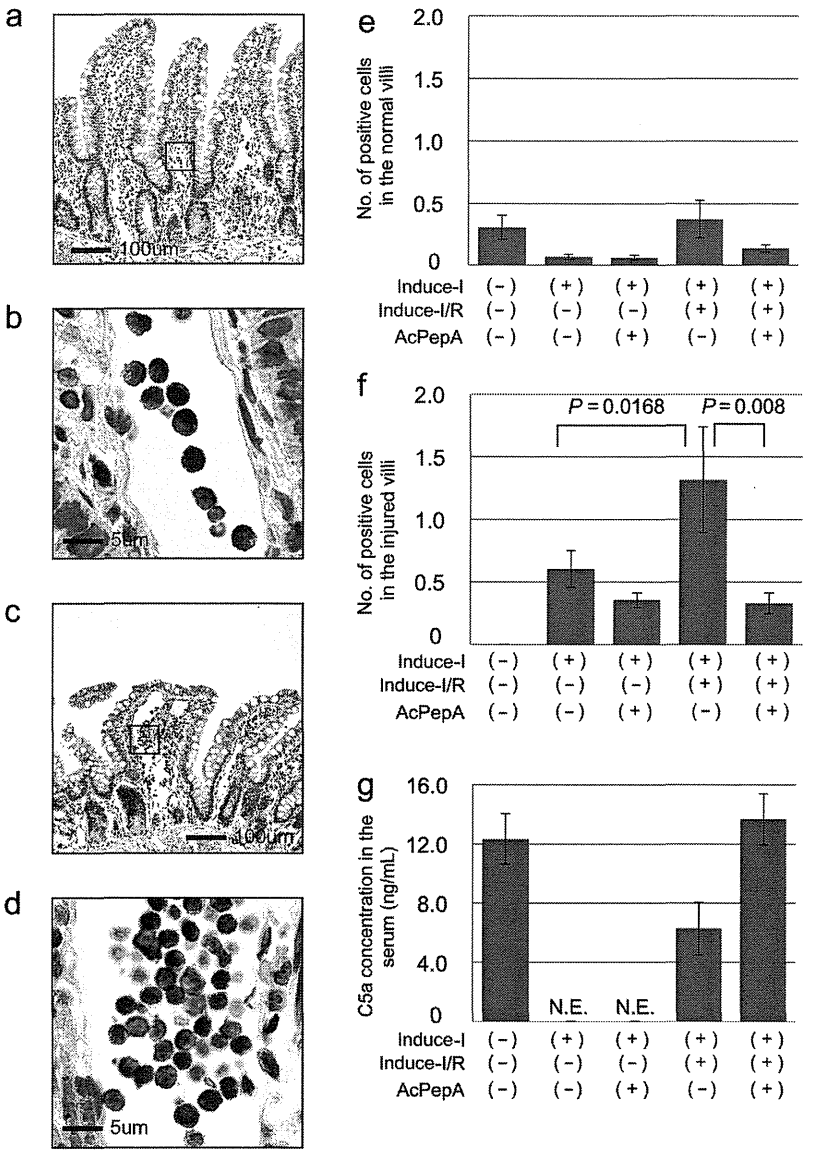

Fig. 3. Induction of C5L2-positive cells in villi. (a) Circulating inflammatory cells are often visible in dilated vessels located in the centers of the villi, this being associated with an inflammatory response (Square in 3a). (b) C5L2-positive cells among inflammatory cells in vessels. (c, d), C5L2-positive cells are also present in dilated vessels in severely injured villi. (e, f) The number of C5L2-positive cells in (e) normal and in (f) injured villi. (g) C5a serum concentrations were significantly lower in the Induce-I/R group than in the Induce-I/R + AcPepA group.

in each normal villus (Fig. 4d). In the injured villi, Induce-I/R significantly increased the number of macrophages, this effect being significantly suppressed by subsequent AcPepA administration (Fig. 4e). These results indicate that CD68+MACs are induced in the small intestine in association with I/R and play a direct role in I/R injury in a manner that is dependent on C5a activation.

Induction of CD204-positive macrophages in villi

CD204-positive macrophages are known to modulate inflammation by producing various cytokines; accordingly, their induction in villi was investigated. These cells were observed not only in stromal lesions outside vessels in slightly injured villi (arrowheads in Fig. 5a), but also infiltrating the erosion fronts of severely injured villi (Fig. 5b). Fewer CD204+MACs were observed in the Induce-I/R + AcPepA than in the Induce-I/R group (Fig. 5c), indicating that inhibition of C5a by AcPepA suppresses activation of macrophages. A mean of approximately one CD204+MAC was present in each control and uninjured villus (Fig. 5d). The average number of CD204+MACs was significantly larger in the uninjured villi of the Induce-I/R group than in those of the controls; additionally, AcPepA significantly decreased the number of CD204+MACs (Fig. 5d). In the injured villi, Induce-I/R induced significantly more numerous CD204+MACs than in the Induce-I alone

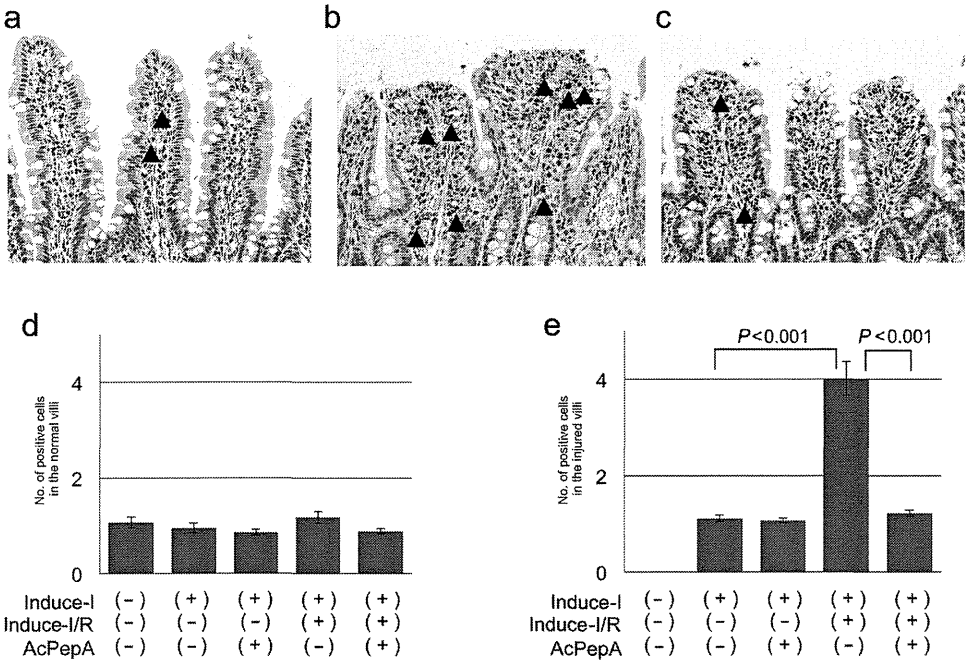

Fig. 4. Induction of macrophages in villi. (a) CD68-positive macrophages are present in the stromal region outside vessels in the villi (arrowheads). (b) CD68-positive macrophages are present in the erosion fronts of injured villi of rats in which I/R was induced (arrowheads). (c) Fewer macrophages are present in the Induce-I/R + AcPepA group. Numbers of the macrophages in (d) normal villi and (e) injured villi.

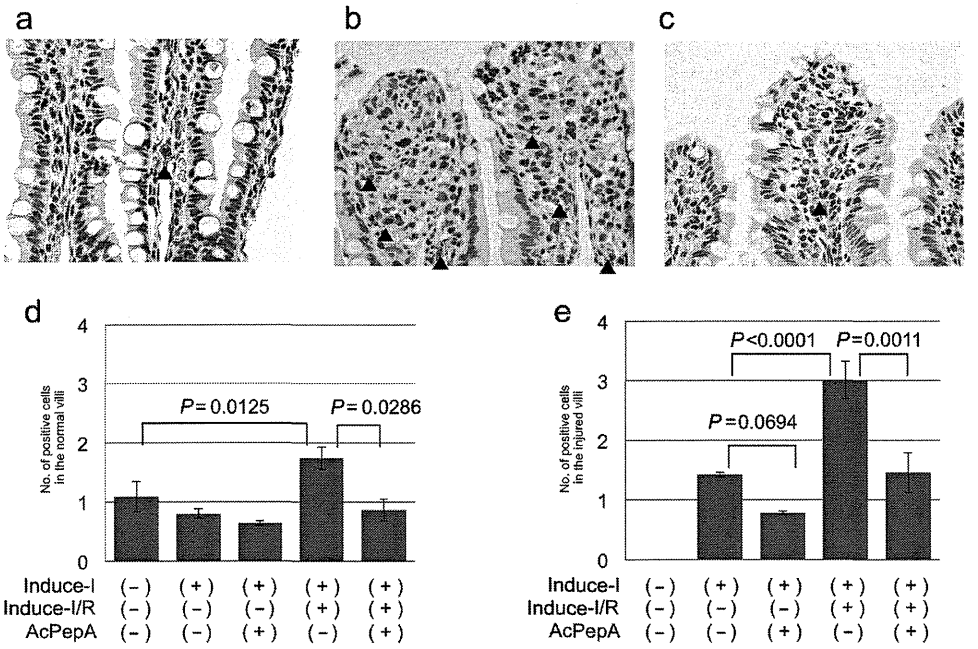

Fig. 5. Induction of CD204-positive macrophages in villi. (a) CD204-positive macrophages are present in the stromal region outside vessels in slightly injured villi (arrowheads). (b) CD204-positive macrophages are present in the erosion fronts of severely injured villi. (c) Fewer CD204-positive macrophages are present in the Induce-I/R + AcPepA group than in the Induce-I/R group. The number of CD204-positive macrophages in (d) normal and (e) injured villi.

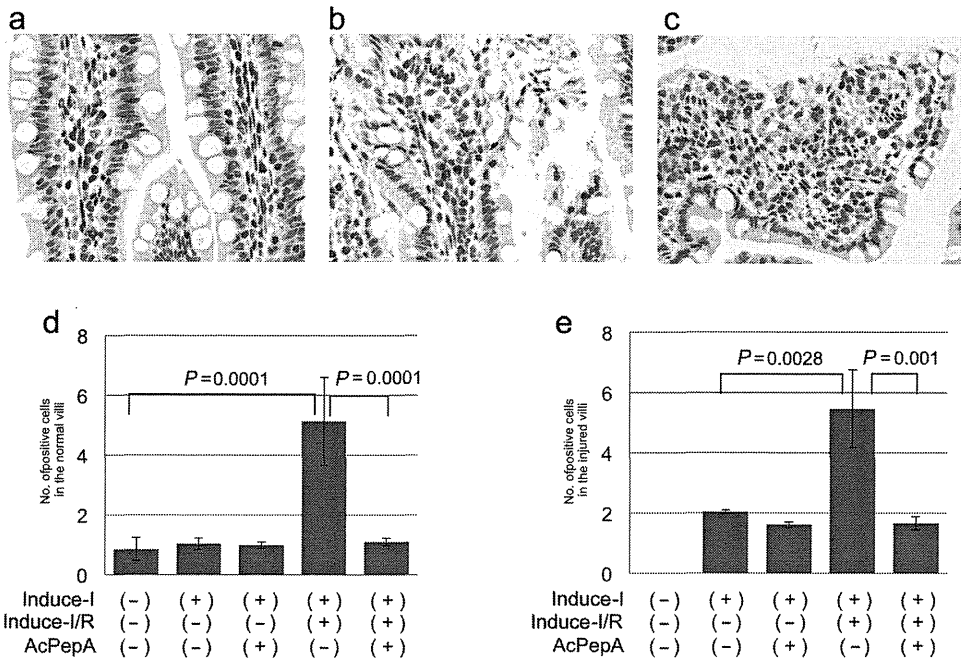

Fig. 6. Induction of HIF1-positive cells. (a, b) HIF1-α-positive cells are present in the stromal regions outside vessels in both (a) slightly injured and (b) moderately injured villi. (c) Many HIF1-α-positive cells are present in the erosion fronts of severely injured villi. (d, e) Changes in numbers of HIF1-α-positive cells in (d) normal and (e) injured villi.

group (Fig. 5e). There were significantly fewer positive cells in the AcPepA with Induce-I/R than in the Induce-I/R group alone; thus, again AcPepA with Induce-I tended to decrease their numbers (Fig. 5e). These results indicate that I/R induces significant CD204+MAC activation in injured villi and suggest that M2-type macrophages may contribute to I/R damage.

Induction of HIF-1α-positive cells

Hypoxia-induced factor 1-alpha is up-regulated in association with ischemic conditions. Therefore, whether HIF1-α-positive cells are involved in I/R-induced changes in the villi was investigated. HIF1-α-positive cells were detected by IHC both in stromal lesions outside vessels in slightly injured villi (Fig. 6a) and in moderately injured villi (Fig. 6b). Many HIF1-α-positive cells were observed in the erosion fronts of severely injured villi (Fig. 6c). The average number of HIF1-α-positive cells was similar to that of CD204+MACs in control, uninjured (Fig. 6d) and injured villi (Fig. 6e), suggesting that CD204+MACs produce HIF1-α.

DISCUSSION

Acute mesenteric ischemia is a serious multifactorial condition that develops from an occlusion of a main artery or vein. Interruption to the intestinal blood flow can lead to macro- and micro-circulatory failure of abrupt onset, frequently resulting in bowel necrosis (4). In this study, we designed an experimental setup for inducing severe injuries based on an AMI model that we had used previously (30–32). Similarly to in ileal specimens from AMI patients (33, 34), in our rat model we observed patchy evidence of damage to the villous mucosa, including detachment of cells, particularly in the villi's apical regions, giving rise to degraded mature epithelial cells in their lumens. We therefore evaluated the effects of I/R and the consequences of using a C5a antagonist to treat epithelial injury and examined regeneration using a clinically relevant experimental AMI protocol.

Acute mesenteric ischemia induces not only structural damage and circulatory deficiencies, but also leads to a great abundance of inflammatory mediators that can result in multi-organ failure (35). The complement system has been demonstrated to be a crucial mediator of I/R injury (36, 37). In the present study, we applied a newly synthesized C5a antagonist peptide, AcPepA (25, 27) and found that it significantly decreased the degree of I/R injury in our AMI model. Thus, we confirmed that C5a is involved in I/R injury in this model.

Because the C5a antagonist peptide AcPepA significantly decreased the degree of I/R damage in this study, we postulated that both structural damage to the villi and

repair of their intestinal epithelial cells would be induced by the inflammatory cytokines released from cells stimulated with C5a generated following complement activation. We therefore examined the cell proliferation activity of intestinal epithelial cells in normal and injured villi by counting the number of proliferating cells visualized by PCNA staining and found that AcPepA significantly increased proliferation of intestinal epithelial cells in injured villi. These results indicate that C5a restriction by AcPepA suppresses cytokine production by inflammatory cells, resulting in suppression of inflammation; any remaining C5a may have directly stimulated the growth of epithelial cells.

We have previously determined the localization of the C5a receptor C5L2 (38) to investigate how C5a/C5L2-mediated signaling modulates the inflammatory responses that lead to I/R injury (39, 40). It has been demonstrated *in vitro* that C5L2 is expressed in neutrophils, macrophages and fibroblasts (41). Additionally, C5a has been shown to exert a chemotactic effect on neutrophils (42), releasing superoxide anions from them. Thus, C5a is believed to be largely responsible for exacerbating PMN-mediated I/R tissue injuries. In the present study, C5a serum concentrations were decreased although C5L2+ PMNs were significantly more numerous in the Induce-I/R group, indicating that serum C5a is consumed because of greater binding to C5L2. It is also possible that the generated C5a is inactivated by carboxypeptidase R (28, 29), also known as thrombin activatable fibrinolysis inhibitor, which removes the carboxy-terminal arginine of C5a causing inactivation of the molecule, resulting in C5a-desArg. However, C5L2 + PMNs were observed mainly in vessels of the villi, a location somewhat distant from the site of epithelial injury. Thus, these results suggest that C5a/C5L signaling has an indirect influence on I/R damage. On the other hand, C5a has been shown to enhance release of pro-inflammatory cytokines from activated macrophages and monocytes (22, 43). Previous studies have suggested that alveolar macrophage activation is a key initiation signal for acute lung I/R injury (44, 45), whereas studies of complement inhibition in mice have suggested that intestinal I/R injury is unaffected by neutrophil depletion (36, 46). We found that CD68+MACs were significantly more numerous after I/R and decreased in number after subsequent AcPepA treatment. In addition, we mainly observed CD68+MACs near the site of injury. Taken together, even though there is some controversy about the direct contribution of neutrophils, C5a has an effect on PMNs and the subsequent activation of macrophages plays an important role in small intestinal I/R injury.

Several studies have demonstrated that M2 type macrophages produce cytokines such as TNF-α, IL-6 and IL-12 in response to inflammatory stimuli (47–49); M2 macrophages are considered to be important effectors of fatal cellular mechanisms during cancer-related inflammation. CD204, a class A scavenger receptor, is a multifunctional molecule that is expressed in M2 macrophages. We postulated that CD204+MACs, which produce HIF1-α, are involved in I/R injury. In the present study, I/R treatment significantly increased the number of CD204+MACs in both injured and normal villi. Again, this increase was suppressed by AcPepA treatment, which suggests that CD204+MACs are indeed activated in response to I/R.

Hypoxia-induced factor 1-alpha is a heterodimeric transcription factor composed of a constitutively expressed alpha-subunit (50) and is important for promoting a variety of cellular responses to hypoxia (51). Induce-I/R would be expected to activate HIF1-α; however, its role in I/R injury is controversial. The protective role of HIF1-α in I/R injury has been demonstrated in proximal tubule cells in the kidney (52--54) as well as in astrocytes (55); additionally, HIF1- α expression is known to be essential for the development of I/R injury in the gut, especially with prolonged ischemia (56, 57). In the present study, I/R significantly increased the number of HIF1-α-positive cells in both injured and uninjured villi. Induction of CD204+MACs correlated closely with the number of HIF1-α-positive cells and both types of cells were suppressed by AcPepA treatment. These results suggest that, on activation with treatment I/R, C5a directly or indirectly induces activation of CD204+MACs in the intestinal villi; these cells then secrete HIF1-α.

The mechanisms for I/R injury involve cellular/molecular processes that begin with hypoxia and hypoxia-induced C5a formation; concerted communication between C5a, MACs and PMNs is necessary for the mediation of I/R damage in the villi. We propose that activated leukocytes flowing into the villus microcirculation spread signals further towards resident macrophages in the lamina propria and that this leads to stimulation of macrophage-derived HIF-1α production at the injury site. According to the outlined scenario, the greatest structural destruction would be expected to occur when C5a, activated PMNs and MACs are all present in the reperfused villi. Furthermore, this cellular casting might also explain the patchy pattern of mucosal damage; the damage is less severe if one or more of the players is not present or inactive.

Several studies have used blocking antibodies or inhibitors to target C5 or C5a. In I/R models of rat intestine, both C5 and C5a blockade result in protection

from I/R injury (16, 58, 59). In myocardial infarcts in rats, antibodies to C5 significantly inhibit necrosis, cell apoptosis and neutrophil infiltration (60). In pigs, use of antibodies directed against C5a results in reduced myocardial injury and reduced coronary endothelial dysfunction after I/R (61, 62). AcPepA, which we generated as an inhibitory C5a peptide, is effective in reducing the incidence of lethal shock in rats (25) and mice (27), as well as sepsis induced by lethal doses of bacterial LPS in cynomolgus monkeys (26). In the present study, we demonstrated that AcPepA suppressed I/R tissue injury in our AMI rat model. Combined together, targeting C5/C5a may represent the best strategy for inhibiting complement-mediated I/R-induced tissue injury and may therefore prove useful for therapeutic interventions in clinical settings. These experimental studies should lead to clinical trials in patients with AMI, lethal shock and sepsis.

In summary, we examined the mechanisms of C5a-induced I/R injury using our clinically relevant rat AMI model. The proposed mechanism includes the effect of C5a on PMNs and the subsequent induction of CD204+MACs, which secrete HIF1-α, in the intestinal villi. Overall, targeting of C5/C5a is a potential strategy for inhibiting PMNs and reducing macrophage- mediated I/R injury and may therefore be a good option for future therapeutic interventions.

ACKNOWLEDGEMENTS

The authors are grateful to Nikolett Beretka, Csilla Mester, Anita Németh, Károly Tóth and Kálmán Vas for their skillful assistance. The study was supported by Hungarian Science Research Fund (OTKA) grants K104656 and Social Renewal Operational Programme (TÁMOP)-4.2.2/A-11/1/KONV-2012-0035 and a grant in aid for JST Research Grant A-STEP (AS2316910G) and Scientific Support Programs for Cancer Research Grant-in-Aid for Scientific Research on Innovative Areas Ministry of Education, Culture, Sports, Science and Technology in Japan.

DISCLOSURE

The authors have no conflict of interest to declare.

REFERENCES

1. Wilson C., Gupta R., Gilmour, D.G., Imrie, C.W. (1987) Acute superior mesenteric ischaemia. *Br J Surg* **74**: 279–81.
2. Oldenburg W.A., Lau L.L., Rodenberg T.J., Edmonds H.J., Burger, C.D. (2004) Acute mesenteric ischemia: A clinical review. *Arch Intern Med* **164**: 1054–62.
3. Benjamin E., Oropello, J.M., Iberti, T.J. (1993) Acute mesenteric ischemia: pathophysiology, diagnosis, and treatment. *Dis Mon* **39**: 131–210.
4. Berland T., Oldenburg W.A. (2008) Acute mesenteric ischemia. *Curr Treat Options Gastroenterol* **11**: 3–10.
5. Rijke R.P., Van Der Meer-Fieggen W., Galjaard H. (1974) Effect of villus length on cell proliferation and migration in small intestinal epithelium. *Cell Tissue Kinet* **7**: 577–86.
6. Yasue N., Guth P.H. (1988) Role of exogenous acid and retransfusion in hemorrhagic shock-induced gastric lesions in the rat. *Gastroenterology* **94**: 1135–43.
7. Noda T., Iwakiri R., Fujimoto K., Matsuo S., Aw, T.Y. (1998) Programmed cell death induced by ischemia-reperfusion in rat intestinal mucosa. *Am J Physiol* **274**: G270–6.
8. Ikeda H., Suzuki Y., Suzuki M., Koike M., Tamura J., Tong J., Nomura M., Itoh G. (1998) Apoptosis is a major mode of cell death caused by ischaemia and ischaemia/reperfusion injury to the rat intestinal epithelium. *Gut* **42**: 530–7.
9. Carter M.B., Wilson M.A., Wead W.B., Garrison R.N. (1996) Platelet-activating factor mediates pulmonary macromolecular leak following intestinal ischemia-reperfusion. *J Surg Res* **60**: 403–8.
10. Yao Y.M., Sheng Z.Y., Yu Y., Tian H.M., Wang Y.P., Lu L.R., Xu S.H. (1995) The potential etiologic role of tumor necrosis factor in mediating multiple organ dysfunction in rats following intestinal ischemia-reperfusion injury. *Resuscitation* **29**: 157–68.
11. Tamion F., Richard V., Lyoumi S., Daveau M., Bonmarchand G., Leroy J., Thuillez C., Lebreton J.P. (1997) Gut ischemia and mesenteric synthesis of inflammatory cytokines after hemorrhagic or endotoxic shock. *Am J Physiol* **273**: G314–21.
12. Parks D.A., Bulkley G.B., Granger D.N., Hamilton S.R., McCord J.M. (1982) Ischemic injury in the cat small intestine: Role of superoxide radicals. *Gastroenterology* **82**: 9–15.
13. Riedemann N.C., Ward P.A. (2003) Complement in ischemia reperfusion injury. *Am J Pathol* **162**: 363–7.
14. Heller T., Hennecke M., Baumann U., Gessner J.E., Zu Vilsendorf A.M., Baensch M., Boulay F., Kola A., Klos A., Bautsch W., Kohl J. (1999) Selection of a C5a receptor antagonist from phage libraries attenuating the inflammatory response in immune complex disease and ischemia/reperfusion injury. *J Immunol* **163**: 985–94.
15. Kimura T., Andoh A., Fujiyama Y., Saotome T., Bamba T. (1998) A blockade of complement activation prevents rapid intestinal ischaemia-reperfusion injury by modulating mucosal mast cell degranulation in rats. *Clin Exp Immunol* **111**: 484–90.
16. Wada K., Montalto M.C., Stahl G.L. (2001) Inhibition of complement C5 reduces local and remote organ injury after intestinal ischemia/reperfusion in the rat. *Gastroenterology* **120**: 126–33.
17. Van Beek J., Bernaudin M., Petit E., Gasque P., Nouvelot, A., Mackenzie E.T., Fontaine M. (2000) Expression of receptors for complement anaphylatoxins C3a and C5a following permanent focal cerebral ischemia in the mouse. *Exp Neurol* **161**: 373–82.
18. Bremer C., Bradford B.U., Hunt K.J., Knecht K.T., Connor H.D., Mason R.P., Thurman R.G. (1994) Role of Kupffer cells in the pathogenesis of hepatic reperfusion injury. *Am J Physiol* **267**: G630–6.
19. Henrion J. (2000) Ischemia/reperfusion injury of the liver: pathophysiologic hypotheses and potential relevance to human hypoxic hepatitis. *Acta Gastroenterol Belg* **63**: 336–47.
20. Wanner G.A., Ertel W., Muller P., Hofer Y., Leiderer R., Menger M.D., Messmer K. (1996) Liver ischemia and

reperfusion induces a systemic inflammatory response through Kupffer cell activation. *Shock* **5**: 34–40.
21. Cavaillon J.M., Fitting C., Haeffner-Cavaillon N. (1990) Recombinant C5a enhances interleukin 1 and tumor necrosis factor release by lipopolysaccharide-stimulated monocytes and macrophages. *Eur J Immunol* **20**: 253–7.
22. Haynes D.R., Harkin D.G., Bignold L.P., Hutchens M.J., Taylor S.M., Fairlie D.P. (2000) Inhibition of C5a-induced neutrophil chemotaxis and macrophage cytokine production *in vitro* by a new C5a receptor antagonist. *Biochem Pharmacol* **60**: 729–33.
23. Tyagi S., Klickstein L.B., Nicholson-Weller A. (2000) C5a-stimulated human neutrophils use a subset of beta2 integrins to support the adhesion-dependent phase of superoxide production. *J Leukoc Biol* **68**: 679–86.
24. Okada N., Imai M., Okada A., Ono F., Okada H. (2011) HMGB1 release by C5a anaphylatoxin is an effective target for sepsis treatment. *natureprecedings* hdl:10101/npre.2011.5727.1.
25. Fujita E., Farkas I., Campbell W., Baranyi L., Okada H., Okada N. (2004) Inactivation of C5a anaphylatoxin by a peptide that is complementary to a region of C5a. *J Immunol* **172**: 6382–7.
26. Okada H., Imai M., Ono F., Okada A., Tada T., Mizue Y., Terao K., Okada N. (2011) Novel complementary peptides to target molecules. *Anticancer Res* **31**: 2511–6.
27. Okada N., Asai, S., Hotta A., Miura N., Ohno N., Farkas I., Hau, L., Okada H. (2007) Increased inhibitory capacity of an anti-C5a complementary peptide following acetylation of N-terminal alanine. *Microbiol Immunol* **51**: 439–43.
28. Campbell W., Okada H. (1989) An arginine specific carboxypeptidase generated in blood during coagulation or inflammation which is unrelated to carboxypeptidase N or its subunits. *Biochem Biophys Res Commun* **162**: 933–9.
29. Campbell W.D., Lazoura E., Okada N., Okada H. (2002) Inactivation of C3a and C5a octapeptides by carboxypeptidase R and carboxypeptidase *N*. *Microbiol Immunol* **46**: 131–4.
30. Szabo A., Vollmar B., Boros M., Menger, M.D. (2008) *In vivo* fluorescence microscopic imaging for dynamic quantitative assessment of intestinal mucosa permeability in mice. *J Surg Res* **145**: 179–85.
31. Boros M., Ghyczy M., Erces D., Varga, G., Tokes T., Kupai, K., Torday C., Kaszaki J. (2012) The anti-inflammatory effects of methane. *Crit Care Med* **40**: 1269–78.
32. Adamicza A., Kaszaki J., Boros M., Hantos Z. (2012) Pulmonary mechanical responses to intestinal ischaemia-reperfusion and endotoxin preconditioning. *Acta Physiol Hung* **99**: 289–301.
33. Chiu C.J., Mcardle A.H., Brown R., Scott H.J., Gurd F.N. (1970) Intestinal mucosal lesion in low-flow states. I. A morphological, hemodynamic, and metabolic reappraisal. *Arch Surg* **101**: 478–83.
34. Thuijls G., Van Wijck K., Grootjans J., Derikx J.P., Van Bijnen A.A., Heineman E., Dejong C.H., Buurman W.A., Poeze M. (2011) Early diagnosis of intestinal ischemia using urinary and plasma fatty acid binding proteins. *Ann Surg* **253**: 303–8.
35. Roumen R.M., Redl H., Schlag G., Zilow G., Sandtner W., Koller W., Hendriks T., Goris R.J. (1995) Inflammatory mediators in relation to the development of multiple organ failure in patients after severe blunt trauma. *Crit Care Med* **23**: 474–80.
36. Austen W.G., Jr., Kyriakides C., Favuzza J., Wang Y., Kobzik L., Moore F.D., Jr., Hechtman H.B. (1999) Intestinal ischemia-reperfusion injury is mediated by the membrane attack complex. *Surgery* **126**: 343–8.
37. De Vries B., Kohl J., Leclercq W.K., Wolfs T.G., Van Bijnen A.A., Heeringa P., Buurman W.A. (2003) Complement factor C5a mediates renal ischemia-reperfusion injury independent from neutrophils. *J Immunol* **170**: 3883–9.
38. Bamberg C.E., Mackay C.R., Lee H., Zahra D., Jackson J., Lim Y.S., Whitfeld P.L., Craig S., Corsini E., Lu B., Gerard C., Gerard N.P. (2010) The C5a receptor (C5aR) C5L2 is a modulator of C5aR-mediated signal transduction. *J Biol Chem* **285**: 7633–44.
39. Hawlisch H., Belkaid Y., Baelder R., Hildeman D., Gerard C., Kohl J. (2005) C5a negatively regulates toll-like receptor 4-induced immune responses. *Immunity* **22**: 415–26.
40. Hopken U.E., Lu B., Gerard N.P., Gerard C. (1996) The C5a chemoattractant receptor mediates mucosal defence to infection. *Nature* **383**: 86–9.
41. Chen N.J., Mirtsos C., Suh D., Lu Y.C., Lin W.J., Mckerlie C., Lee T., Baribault H., Tian H., Yeh W.C. (2007) C5L2 is critical for the biological activities of the anaphylatoxins C5a and C3a. *Nature* **446**: 203–7.
42. Shin H.S., Snyderman R., Friedman E., Mellors A., Mayer M.M. (1968) Chemotactic and anaphylatoxic fragment cleaved from the fifth component of guinea pig complement. *Science* **162**: 361–3.
43. Okusawa S., Yancey K.B., Van Der Meer J.W., Endres S., Lonnemann G., Hefter K., Frank M.M., Burke J.F., Dinarello C.A., Gelfand J.A. (1988) C5a stimulates secretion of tumor necrosis factor from human mononuclear cells *in vitro*. Comparison with secretion of interleukin 1 beta and interleukin 1 alpha. *J Exp Med* **168**: 443–8.
44. Amaral F.A., Fagundes C.T., Guabiraba R., Vieira A.T., Souza A.L., Russo R.C., Soares M.P., Teixeira M.M., Souza D.G. (2007) The role of macrophage migration inhibitory factor in the cascade of events leading to reperfusion-induced inflammatory injury and lethality. *Am J Pathol* **171**: 1887–93.
45. Zhao M., Fernandez L.G., Doctor A., Sharma A.K., Zarbock A., Tribble C.G., Kron I.L., Laubach V.E. (2006) Alveolar macrophage activation is a key initiation signal for acute lung ischemia-reperfusion injury. *Am J Physiol Lung Cell Mol Physiol* **291**: L1018–26.
46. Rehrig S., Fleming S.D., Anderson J., Guthridge J.M., Rakstang J., Mcqueen C.E., Holers V.M., Tsokos G.C., Shea-Donohue T. (2001) Complement inhibitor, complement receptor 1-related gene/protein y-Ig attenuates intestinal damage after the onset of mesenteric ischemia/reperfusion injury in mice. *J Immunol* **167**: 5921–7.
47. Haworth R., Platt N., Keshav S., Hughes D., Darley E., Suzuki H., Kurihara Y., Kodama T., Gordon S. (1997) The macrophage scavenger receptor type A is expressed by activated macrophages and protects the host against lethal endotoxic shock. *J Exp Med* **186**: 1431–9.
48. Beamer C.A., Holian A. (2005) Scavenger receptor class A type I/II (CD204) null mice fail to develop fibrosis following silica exposure. *Am J Physiol Lung Cell Mol Physiol* **289**: L186–95.
49. Coller S.P., Paulnock D.M. (2001) Signaling pathways initiated in macrophages after engagement of type A scavenger receptors. *J Leukoc Biol* **70**: 142–8.
50. Semenza G.L. (2001) HIF-1 and mechanisms of hypoxia sensing. *Curr Opin Cell Biol* **13**: 167–71.
51. Weidemann A., Johnson R.S. (2008) Biology of HIF-1alpha. *Cell Death Differ* **15**: 621–7.
52. Bernhardt W.M., Campean V., Kany S., Jurgensen J.S., Weidemann A., Warnecke C., Arend M., Klaus S., Gunzler V., Amann K., Willam C., Wiesener M.S., Eckardt K.U. (2006) Preconditional activation of hypoxia-inducible factors

ameliorates ischemic acute renal failure. *J Am Soc Nephrol* **17**: 1970–8.
53. Hill P., Shukla D., Tran M.G., Aragones J., Cook H.T., Carmeliet P., Maxwell P.H. (2008) Inhibition of hypoxia inducible factor hydroxylases protects against renal ischemia-reperfusion injury. *J Am Soc Nephrol* **19**: 39–46.
54. Manotham K., Tanaka T., Ohse T., Kojima I., Miyata T., Inagi R., Tanaka H., Sassa R., Fujita T., Nangaku M. (2005) A biologic role of HIF-1 in the renal medulla. *Kidney Int* **67**: 1428–39.
55. Du F., Zhu L., Qian Z.M., Wu X.M., Yung W.H., Ke Y. (2010) Hyperthermic preconditioning protects astrocytes from ischemia/reperfusion injury by up-regulation of HIF-1 alpha expression and binding activity. *Biochim Biophys Acta* **1802**: 1048–53.
56. Sutton T.A., Wilkinson J., Mang H.E., Knipe N.L., Plotkin Z., Hosein M., Zak K., Wittenborn J., Dagher P.C. (2008) p53 regulates renal expression of HIF-1{alpha} and pVHL under physiological conditions and after ischemia-reperfusion injury. *Am J Physiol Renal Physiol* **295**: F1666–77.
57. Feinman R., Deitch E.A., Watkins A.C., Abungu B., Colorado I., Kannan K.B., Sheth S.U., Caputo F.J., Lu Q., Ramanathan M., Attan S., Badami C.D., Doucet D., Barlos D., Bosch-Marce M., Semenza G.L., Xu D.Z. (2010) HIF-1 mediates pathogenic inflammatory responses to intestinal ischemia-reperfusion injury. *Am J Physiol Gastrointest Liver Physiol* **299**: G833–43.
58. Arumugam T.V., Shiels I.A., Woodruff T.M., Reid R.C., Fairlie D.P., Taylor S.M. (2002) Protective effect of a new C5a receptor antagonist against ischemia-reperfusion injury in the rat small intestine. *J Surg Res* **103**: 260–7.
59. Hill J., Lindsay T.F., Ortiz F., Yeh C.G., Hechtman H.B., Moore F.D., Jr. (1992) Soluble complement receptor type 1 ameliorates the local and remote organ injury after intestinal ischemia-reperfusion in the rat. *J Immunol* **149**: 1723–8.
60. Vakeva A.P., Agah A., Rollins S.A., Matis L.A., Li L., Stahl G.L. (1998) Myocardial infarction and apoptosis after myocardial ischemia and reperfusion: Role of the terminal complement components and inhibition by anti-C5 therapy. *Circulation* **97**: 2259–67.
61. Tofukuji M., Stahl G.L., Agah A., Metais C., Simons M., Sellke F.W. (1998) Anti-C5a monoclonal antibody reduces cardiopulmonary bypass and cardioplegia-induced coronary endothelial dysfunction. *J Thorac Cardiovasc Surg* **116**: 1060–8.
62. Amsterdam E.A., Stahl G.L., Pan H.L., Rendig S.V., Fletcher M.P., Longhurst J.C. (1995) Limitation of reperfusion injury by a monoclonal antibody to C5a during myocardial infarction in pigs. *Am J Physiol* **268**: H448–57.

In vivo ^{18}F-fluorodeoxyglucose-positron emission tomography/computed tomography imaging of pancreatic tumors in a transgenic rat model carrying the human *KRAS*^{G12V} oncogene

KOJI SHIBATA[1,2], KATSUMI FUKAMACHI[1], ATSUSHI TSUJI[3], TSUNEO SAGA[3], MITSURU FUTAKUCHI[1], MASATO NAGINO[2], HIROYUKI TSUDA[4] and MASUMI SUZUI[1]

[1]Department of Molecular Toxicology, Nagoya City University Graduate School of Medical Sciences and Medical School, Nagoya, Aichi 467-8601; [2]Division of Surgical Oncology, Department of Surgery, Nagoya University Graduate School of Medicine, Nagoya, Aichi 466-8550; [3]Diagnostic Imaging Program, Molecular Imaging Center, National Institute of Radiological Sciences, Chiba, Chiba 263-8555; [4]Laboratory of Nanotoxicology Project, Nagoya University, Nagoya, Aichi 467-8603, Japan

Received March 25, 2014; Accepted December 19, 2014

DOI: 10.3892/ol.2015.3053

Abstract. A novel *KRAS*-mediated transgenic rat model has previously been demonstrated, in which animals develop multiple pancreatic ductal adenocarcinoma (PDAC) that is histologically similar to human PDAC within two weeks. Positron emission tomography (PET)/computed tomography (CT) is commonly used for the diagnosis and staging of PDAC in humans, and can be adopted for optimal use in animal experiments. The aim of the present study was to evaluate the carcinogenic process in a rat pancreatic carcinoma model using small-animal multimodality imaging systems. The utility of fluorodeoxyglucose (FDG)-PET/CT in detecting the location and size of PDAC during tumor development in the present transgenic rat model was assessed. A small animal multimodality PET/CT system and contrast-enhanced CT (CECT) system were used for the imaging analysis of *KRAS*^{G12V} male transgenic rats (n=6), which developed pancreatic tumors following the administration of an injection of Cre recombinase (Cre)-carrying adenovirus. Laparotomies performed at six weeks post-treatment revealed that all three (100%) Cre-expressing rats developed pancreatic tumors that were <2 mm in diameter, none of which were detected by ^{18}F-FDG PET/CT or CECT. At eight weeks post-treatment, the pancreatic tumors were heterogeneously visualized by ^{18}F-FDG-PET/CT and CECT in two of the three rats. Furthermore, the autopsies confirmed that all three rats had developed pancreatic tumors. These novel findings provide evidence that the FDG-PET/CT imaging system is a valuable tool for the evaluation of the carcinogenic process, and one which may aid in treatment and preventive methods for pancreatic tumors in mammalian models. A limitation associated with the early detection of PDACs warrants further investigation.

Correspondence to: Dr Masumi Suzui, Department of Molecular Toxicology, Nagoya City University Graduate School of Medical Sciences and Medical School, 1 Kawasumi, Mizuho-cho, Mizuho-ku, Nagoya, Aichi 467-8601, Japan
E-mail: suzui@med.nagoya-cu.ac.jp

Key words: carcinogenesis, positron emission tomography/computed tomography, ^{18}F-fluorodeoxyglucose, laparotomy, pancreatic tumor, rat model

Introduction

With >250,000 annual mortalities, pancreatic carcinoma is one of the most lethal malignancies, ranking 12th worldwide (1). Mortality resulting from this disease is high even in developed countries, including Japan, the United Kingdom, France and the United States (2,3). Overall, >75% of pancreatic carcinoma cases are histologically characterized as pancreatic ductal adenocarcinoma (PDAC) (4,5). The majority of cases of PDAC are incurable due to the necessity of extensive resection, which is often not feasible, and due to the fact that the disease is rarely identified at an early stage. Furthermore, the majority of patients with advanced PDAC either do not respond, or respond transiently to chemotherapeutic drugs and radiation (6). Typically, the majority of patients with PDAC succumb to the disease within one year of diagnosis, and the overall five-year survival rate is <5% (7). Even in patients with resectable carcinoma, the long-term outcome remains unsatisfactory due to the incidence of early recurrence following surgical resection.

In order to gain an improved understanding of this lethal malignant carcinoma, studies that use animal PDAC models with pancreatic neoplasms that resemble human PDAC are usually desirable. By focusing on human pancreatic adenocarcinomas that express a high frequency of *KRAS* mutation, a transgenic rat model carrying the human *HRAS*^{G12V} or *KRAS*^{G12V} oncogene was established (8,9). The activation of the target transgene is attained by the injection of a Cre recombinase (Cre)-carrying adenovirus into the pancreatic ducts of the animal via the

common bile duct (8,9). In this model, the transgenic rats usually develop pre-neoplastic and neoplastic pancreatic lesions within two weeks of the viral inoculation (10). These lesions in the transgenic rats exhibit morphological similarities to those observed in human pancreatic lesions, including PDAC (11) and intraepithelial neoplasias (PanINs) (9).

Due to the position of the tumors within the abdominal cavity, laparotomy is the only technique that is able to determine the existence and size of pancreatic tumors within the transgenic rats following virus inoculation, as the tumors cannot be visually assessed from surface scans of the affected rats. A previous study determined that in order to serologically detect early-stage PDAC in the rat models, serum N-ERC levels and the levels of several serum miRNAs, which are expressed differentially in PDAC transgenic rats and control rats, could be used (8,12). However, even in the case of elevated levels of high serum biomarkers, the exact location and size of pancreatic tumors is difficult to detect unless exploratory surgery is performed within the abdominal cavity.

^{18}F-fluorodeoxyglucose-positron emission tomography ([^{18}F-FDG-PET) is commonly used during the diagnosis of pancreatic tumors (13,14). Due to a high sensitivity and penetration depth, PET is considered to be more accurate for the detection and identification of metastases in humans and animal models than other imaging systems (15,16).

The objective of the present study was to evaluate the carcinogenic process in a mammalian model using imaging modalities, such as PET/computed tomography (CT), which are applicable for the study of human PDAC.

Materials and methods

Animals. In total, six male *KRAS*^{G12V} oncogene transgenic rats were used in the present study. Routine genotyping was performed as previously described (8). The rats were kept in plastic cages in an air-conditioned room at 24±2˚C and 60±5% humidity with a 12-h light/12-hour dark cycle. A basal diet (Oriental Yeast Co., Ltd., Tokyo, Japan) and tap water were available *ad libitum* throughout the experiment. All experiments were approved by the Animal Care and Use Committee of Nagoya City University Graduate School of Medical Sciences and the National Institute of Radiological Sciences (Tokyo, Japan).

Procedure of adenovirus inoculation. The preparation and inoculation of the adenoviruses was performed as previously described (9). In brief, a Cre-recombinase expressing adenovirus was amplified in HEK293 cells and then purified using the Vivapure AdenoPACK (Vivascience, Hannover, Germany) (17). The titer of the adenovirus was then determined using an Adeno-X rapid titer kit (Clontech, Mountain View, CA, USA). The virus was prepared to a concentration of 4.0×10^9 plaque-forming units/ml. The virus (300-400 μl) was injected using a small syringe into the pancreatic duct of the rats as previously described (9).

[^{18}F-FDG-PET and CT procedures, and image analysis. The time course of the experimental protocol is shown in Fig. 1. For the present study, 10-week-old male *KRAS*^{G12V} transgenic rats were used. The rats were divided into two groups, with three rats per group. The rats in groups 1 and 2 were administered with the Cre-expressing adenovirus vector or an empty vector (negative control), respectively. A small-animal multimodality PET system (Inveon; Siemens Healthcare Inc., Malvern, PA, USA) was used for PET data acquisition. Following an overnight fast, each rat (body weight, 403-583 g) was injected with 15 MBq (14.6±1.6 MBq) ^{18}F-FDG (Nihon Medi-Physics Co., Ltd., Tokyo, Japan) via the tail vein, whilst the rat was under isoflurane anesthesia. The PET data acquisition was conducted for 10 min, beginning 50 min after the ^{18}F-FDG injection. Using a lamp, the body temperature of the rats was maintained at between 36 and 37˚C during the scan. The images were reconstructed using a 3D maximum *a posteriori* (18 iterations with 16 subsets; β=0.2), without attenuation correction. The tracer uptake was expressed as the standardized uptake value (SUV).

Subsequent to PET scanning, plain or contrast-enhanced CT (CECT) was conducted with an X-ray source set at 90 kVp and 200 μA, using a small-animal CT system (R_mCT2; Rigaku, Tokyo, Japan). For CECT, the rats were intravenously injected with 10 ml Iopamiron 370 contrast medium (Bayer Yakuhin Ltd., Osaka, Japan) using an infusion pump (NE-1000; Neuroscience Inc., Tokyo, Japan) at the rate of 2 ml/min, whilst the rats were under isoflurane anesthesia. The CECT images were acquired 5 min subsequent to the injection. In order to reduce the motion artifacts caused by respiratory and peristaltic movement during the CT scan, a respiratory gating system was used whilst the rats under inhalable isoflurane anesthesia. The ^{18}F-FDG-PET scanning was conducted at two, three, four, five and eight weeks subsequent to administration of the Cre-expressing adenovirus or the empty vectors. In order to confirm the results of the PET analysis, the CECT scan was also conducted at five and eight weeks subsequent to the virus injection. For the quantitative analysis, the PET and CT data sets were imported and the fused images were then obtained using ASIPro VM software (CTI Concorde Microsystems, Knoxville, TN, USA). Laparotomy was performed six weeks subsequent to the injection in order to confirm the location and size of the pancreatic tumors, which were visible to the naked eye. The experimental rats were sacrificed eight weeks subsequent to the injection.

Histopathological examination. The rats in groups 1 and 2 survived until the end of the experimental period. The pancreatic tumors and the normal pancreatic lobes were removed from the abdomen of the rats, fixed with 10% buffered formalin and then processed for histopathological examination using hematoxylin and eosin stain (9). The pancreatic lesions were diagnosed histopathologically based upon previously described criteria (8,9).

Results

PET/CT findings and histopathological examination. The six rats were euthanized eight weeks subsequent to the injection of the Cre-expressing viral or empty vectors. All three Cre-expressing transgenic rats in group 1 (100%) developed orthotopic pancreatic tumors without distant metastasis. By contrast, no tumors were identified in the negative control rats of group 2. Upon macroscopic analysis, the tumors appeared nodular and solid in shape, and were ochre yellow in color. The

Table I. Mean SUV of the tumor and each organ in the experimental rats.

Rat	Tumor (SUV_{max})	GI tract (SUV_{max})	Liver	Kidney (cortex and medulla)
1	0.7-1.2 (1.4)	0.5-1.0 (3.2)	0.4-0.5	0.8-0.9
2	0.9-2.0 (3.0)	0.5-1.8 (2.7)	0.5-0.6	0.9-1.1
3	ND	0.6-1.4 (4.2)	0.6-0.7	0.9-1.1

The rats were inoculated with a Cre recombinase-expressing vector as described in the Materials and methods section. The values were calculated using the scanning data obtained at eight weeks post-inoculation. SUV_{max}, maximum standardized uptake value; GI, gastrointestinal; ND, Not detected.

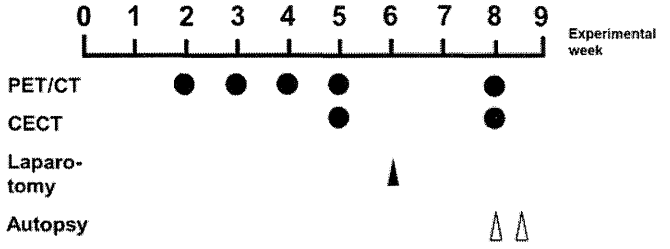

Figure 1. Experimental time course. Closed circle indicates the time of scanning. Closed triangle indicates the time of laparotomy. Open triangle indicates the time of autopsy. Laparotomy and autopsy were performed on the three rats from group 1 at eight weeks post-viral inoculation. Viral inoculation was performed at week zero. PET, positron emission tomography; CT, computed tomography; CECT, contrast-enhanced computed tomgraphy.

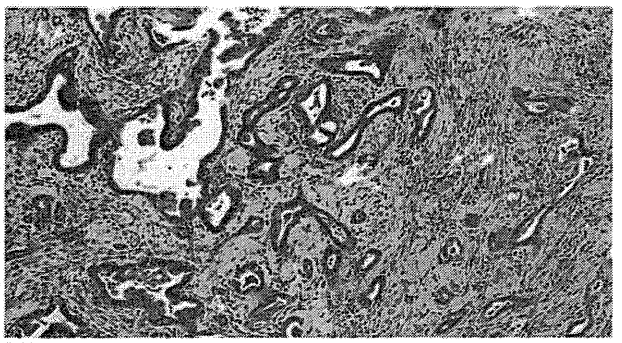

Figure 2. Representative microscopic image of a pancreatic ductal adenocarcinoma, revealing papillotubular growth of the tumor cells and abundant fibrous tissue proliferation (hematoxylin and eosin staining; magnification, x100).

PET/CT images obtained eight weeks subsequent to the viral injection revealed the majority of tumor tissues to be distinguishable from the adjacent organs, but the tissues were challenging to distinguish from the normal intestinal tissues, depending on the site of the tumor. The pancreatic tumors were of the ductal adenocarcinoma histological type. The coexistence of adenocarcinoma and PanIN lesions surrounded by fibrous tissue with inflammatory cell infiltration was also identified (Fig. 2).

[^{18}F-FDG-PET imaging prior to experimental week five. The representative maximal-intensity projection images from ^{18}F-FDG-PET are shown in Fig. 3. PET scanning was performed four times prior to the five experimental weeks. A marginal or very high uptake in the gastrointestinal tract and urinary bladder, which was considered to be physiological FDG uptake, was observed in all three Cre-expressing transgenic rats and three control rats. At five weeks post-treatment, the tumors were not clearly visualized by the indicated imaging system. Following the laparotomy at six weeks post-treatment, a few small nodules measuring between 1 and 2 mm in diameter, indicative of a carcinoma, were identified in the pancreas of all Cre-expressing transgenic rats. No metastases were identified in the rats of the negative control group.

Analysis of CECT, PET and PET/CT images at eight weeks post-treatment. Representative slices of the ^{18}F-FDG-PET/CT fusion images obtained from the Cre-expressing transgenic rats are shown in Figs. 4-6. The SUV_{max} and SUV_{mean} of the pancreatic tumors and each organ are shown in Table I. In rat 1 (body weight, 503 g), the CECT images revealed a heterogeneous lesion measuring 17 mm in the maximum sagittal diameter in the left side of the abdomen. In addition, the PET and PET/CT fusion images revealed moderately increased ^{18}F-FDG uptake in the lesion located in the left side of the abdomen, with a SUV_{max} of <1.5. Physiological FDG uptake was observed in the gastrointestinal tract, and the SUV_{max} of this organ site was 3.2, as shown in Table I. Autopsy revealed a large tumor in the splenic lobe, which was detected by CECT and PET/CT. However, multiple tumors that were present in the duodenal lobe of the pancreas were not revealed by CECT and PET/CT (Fig. 4). In rat 2 (body weight, 470 g), the CECT images revealed a heterogeneously-enhanced pancreatic tumor, measuring 20 mm in the maximum sagittal diameter, in the left side of the abdomen. PET/CT fusion images revealed moderate uptake of ^{18}F-FDG (SUV_{max}, 3.0) in the pancreatic tumor. In addition, physiological FDG uptake in the gastrointestinal tract (SUV_{max}, 2.7) was observed. During autopsy, a large tumor in the splenic lobe was identified by the imaging analysis. In addition, multiple tumors were identified in the duodenal lobe of the pancreas, but these tumors were not visualized on CECT and PET/CT (Fig. 5). In rat 3 (body weight, 564 g), the presence of a tumor was not observed on either CECT or PET scans (Fig. 6). Next, an incision was made in the abdomen of the rat, and a number of nodules, which were smaller in size than those observed in rats no. 1 and 2, were identified in the

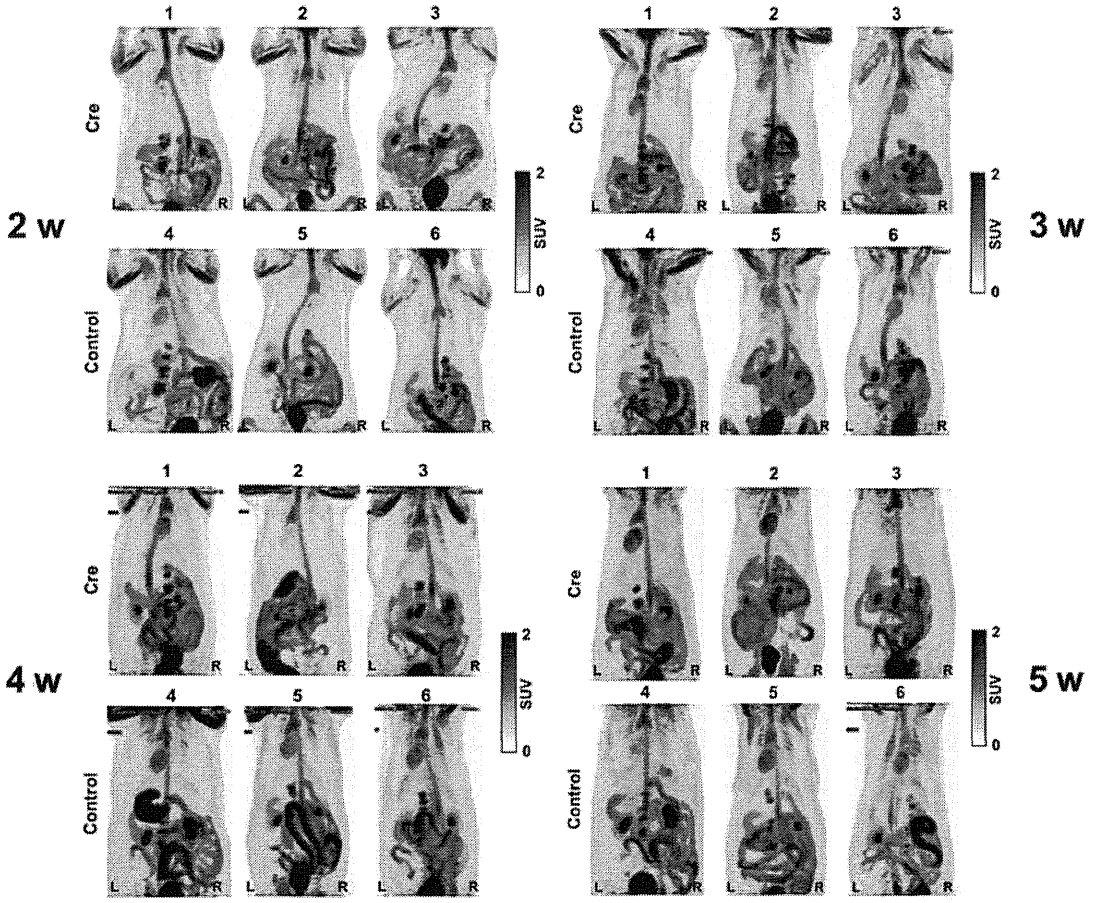

Figure 3. Representative positron emission tomography (PET) images of the transgenic rats at a maximum intensity projection. Images were obtained from Cre recombinase (Cre)-expressing transgenic rats (1-3) and control rats (4-6). Scanning was performed at two, three, four and five weeks post-viral inoculation. Subsequent to fasting, the rats were injected under isoflurane anesthesia with ~15 MBq ^{18}F-fluorodeoxyglucose (FDG) via the tail vein. PET data was acquired 50 min post-injection. Physiological FDG uptake was observed in the intestines, kidney and urinary bladder, but no tumor masses were identified in any of the images. L, left side; R, right side. SUV, standardized uptake value; w, weeks.

duodenal lobe of the pancreas. No tumor was identified in the splenic lobe of the pancreas. No macroscopic metastasis was identified in rats 1-3.

Discussion

A limited number of the documented studies that involve imaging analysis of pancreatic tumors in animal models used the FDG-PET/CT system (18,19). In the present study, a *KRAS*-mediated transgenic rat model was used to develop multiple pancreatic tumors that resembled the developmental and histological features of human PDAC within two weeks (8). In living rats at eight weeks post-treatment, the pancreatic tumors were clearly enhanced in the CECT images following the administration of a contrast media, and were distinguishable from the gastrointestinal tract. In the absence of imaging analysis, calipers are used to determine the location and size of a pancreatic tumor following a laparotomy or autopsy of an animal. Imaging analysis therefore allows each animal to be scanned sequentially in a sectional plane of interest, such as transverse, coronal or sagittal, and be monitored over time without the need to be sacrificed. In addition, PET/CT enables the accurate measurement of irregularly-shaped tumors in a pancreatic tumor model. According to the Three Rs principle (20), which aims to replace existing experimental methods with those that do not use animals, reduce the number of test animals used and refine methods in order to minimize the suffering of test animals, the PET/CT system reduces the number of animals required for experimental treatment and control groups. This indicates that imaging systems should be recommended for use in animal experiments. Recently, inoculation efficacy has been improved by clamping the common bile duct and increasing the amount of virus that is administered. Using this technique, studies may be able to control the size of the pancreatic tumor quantitatively within an appropriate time period, a factor that demonstrates the usefulness of this model.

With regard to studies that have used small animal models, Kitahashi *et al* (21) used micro-CT to detect chemically-induced pancreatic tumors of >4 mm in diameter in Syrian hamsters. Another study by Fendrich *et al* (18) detected precursor pancreatic adenocarcinoma lesions with an activity of 9.6±0.5 MBq in a five-month-old transgenic mouse model by FDG-PET/CT. Kayed *et al* (22) measured the anticancer effects of cyclopamine in a pancreatic carcinoma xenograft with an activity of 7.4 MBq model using ^{18}F-PET/CT. The study examined the size and SUV of each

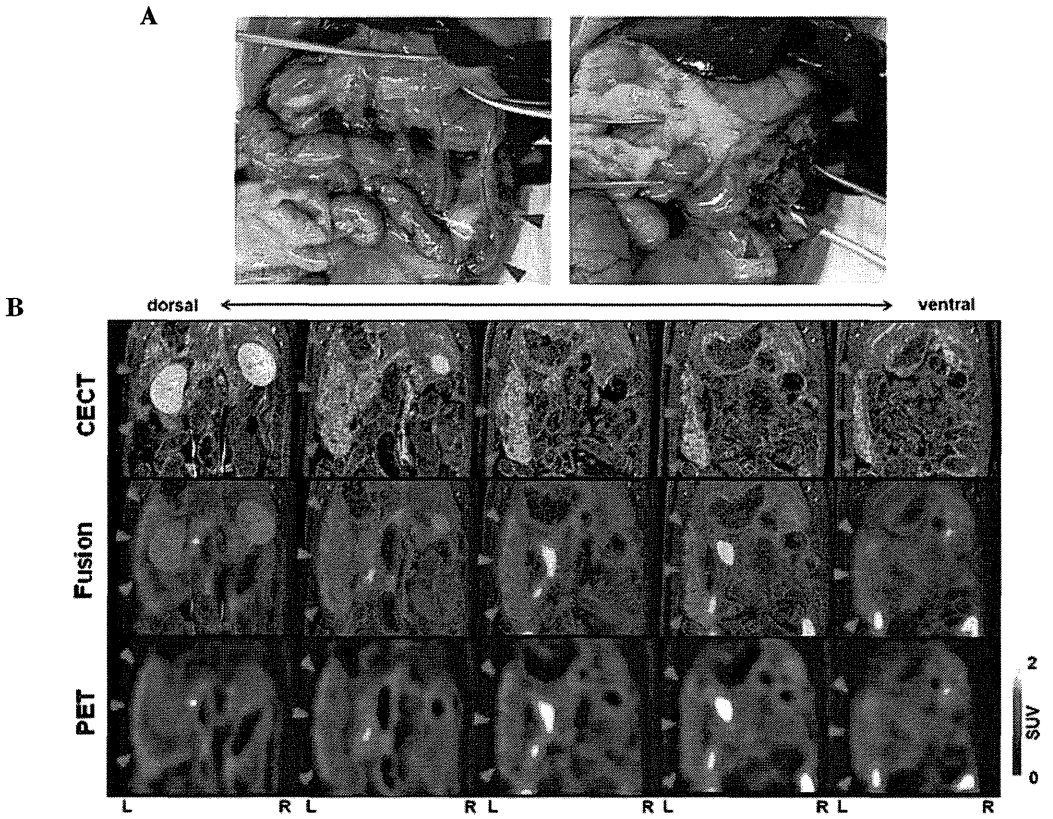

Figure 4. Autopsy view, positron emission tomography (PET)/contrast-enhanced CT (CECT) and PET/CECT fusion images of rat 1. (A) Tumors were observed in the duodenal lobe (left panel, red arrowheads) and the in splenic lobe (left and right panel, blue arrowheads) of the pancreas. (B) PET, CECT and PET/CECT fusion images revealed a large mass on the left side of the body (arrowheads). Physiological fluorodeoxyglucose uptake was also observed in the kidneys and intestines. L, left side; R, right side; SUV, standardized uptake value.

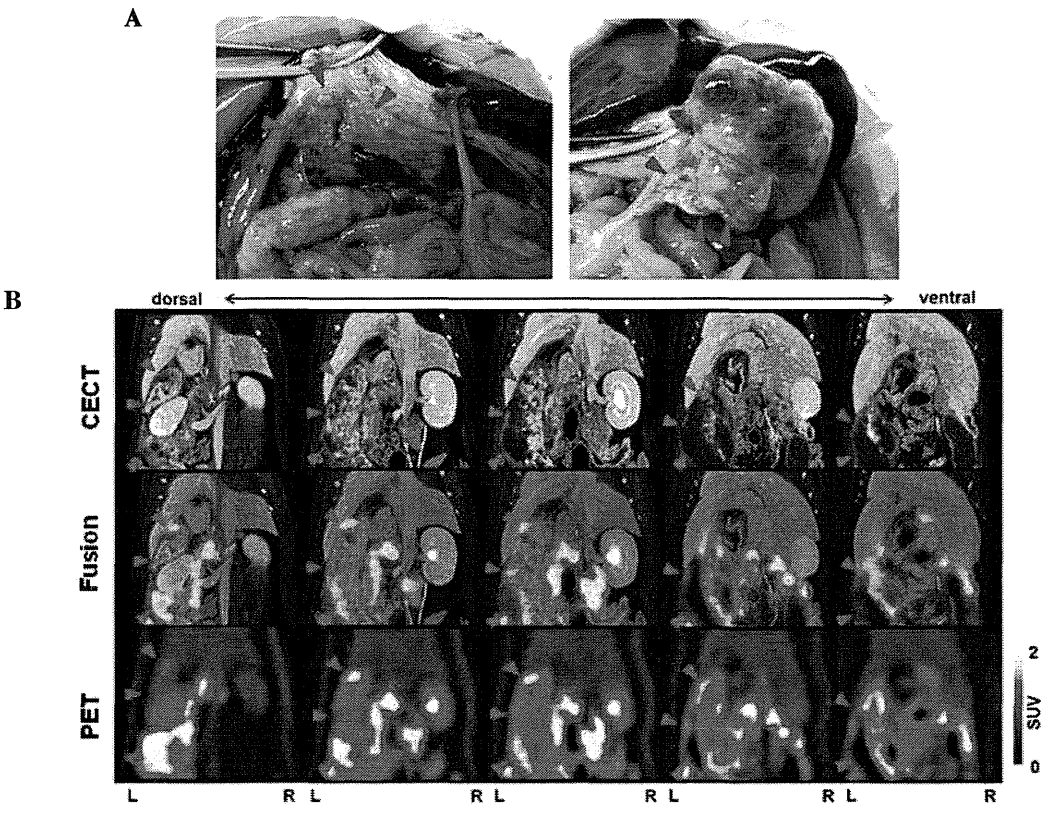

Figure 5. Autopsy view, positron emission tomography (PET), contrast-enhanced CT (CECT) and PET/CECT fusion images of rat 2. (A) Tumors were observed in the duodenal lobe (left and right panels, arrowheads) of the pancreas. The liver was intact. (B) PET, CECT and PET/CECT fusion images revealed multiple tumor masses in the left side of the body (arrowheads). L, left side; R, right side; SUV, standardized uptake value.